Cosmological results from the first three years of observations of the Dark Energy Survey - an overview -

Hugo Camacho

LIneA Webinar
12 Aug 2021

Structure of this talk

- Introduction
  - Cosmology and Dark energy from the large scale structure of the universe.
  - The Dark Energy Survey (DES).
- DES cosmological analysis results
  - From two-point correlation functions of positions and shapes of galaxies.
  - From the angular BAO feature detection.

Concordance/ΛCDM cosmology & cosmic acceleration

Large scales universe description:

Fluid on an expanding background

Acceleration rate

$$\frac{\ddot{a}}{a} = -\frac{4\pi G}{3}\left(\rho + \frac{3p}{c^2}\right) + \frac{\Lambda c^2}{3}$$

Matter, radiation, relativistic species: pressure $p \geqq 0$

scale factor

cosmological constant

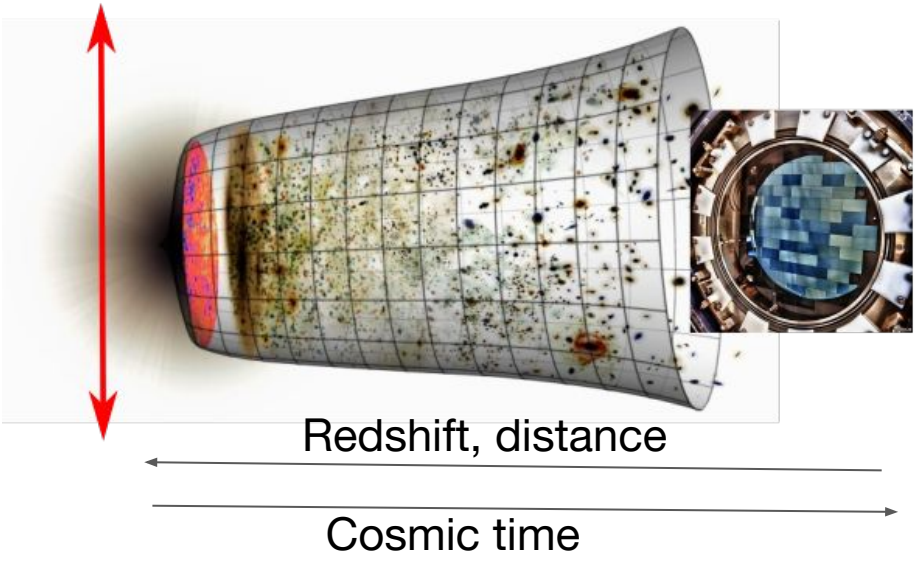

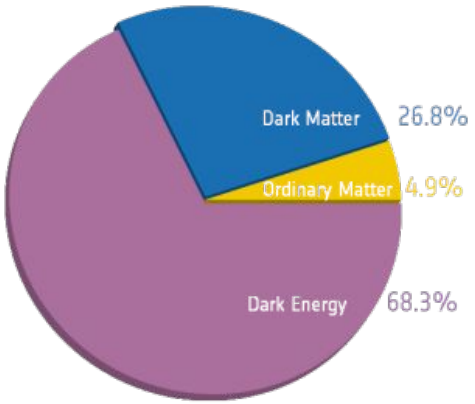

Cosmic acceleration and Dark Energy

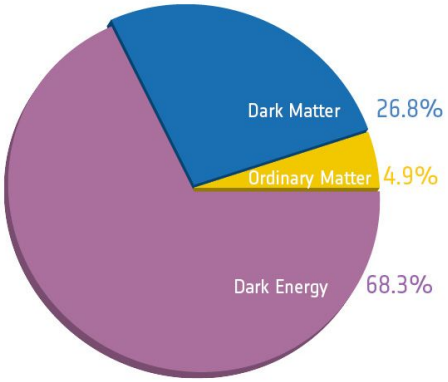

Concordance / fiducial model

- Parameters of this universe:
  - Densities of matter (Ωm ~0.3), dark energy (ΩΛ ~0.7), baryons (~0.05), neutrinos
  - Amplitude of structure σ8 ~0.8
  - Expansion rate h~0.69

- Independent observational evidence
  - Supernovae are further away than expected
  - Growth of structure has been slowed
- Tremendous implications for physics/astronomy
  - Current understanding of gravity is incomplete
  - Current understanding of universe constituents is incomplete

Improving our tests of ΛCDM basic predictions?

Are the **late Universe** and **early Universe** data explained by the **same** model?

Do the **growth** of structure and **expansion** measurements agree?

Does the **Dark Energy density change** with cosmic expansion

"Equation of state" parameter w=pressure/density

The Dark Energy Survey (DES)

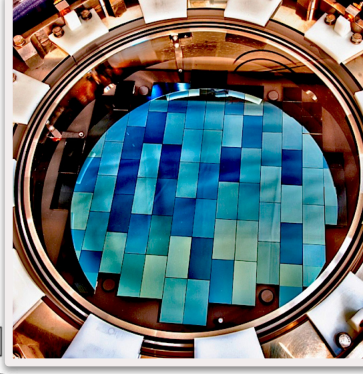

- >400 members, 25 institutions, 7 countries
- 570 Megapixel camera for the Blanco 4m telescope in Chile.
- Full survey, ~5.5Y. 2013-2019 (Y3 2013-16).
- **Wide field:** 5000 sq. deg. in 5 bands grizY. ~23 magnitude.
- DES Y3: Positions and shapes of > 100M galaxies.

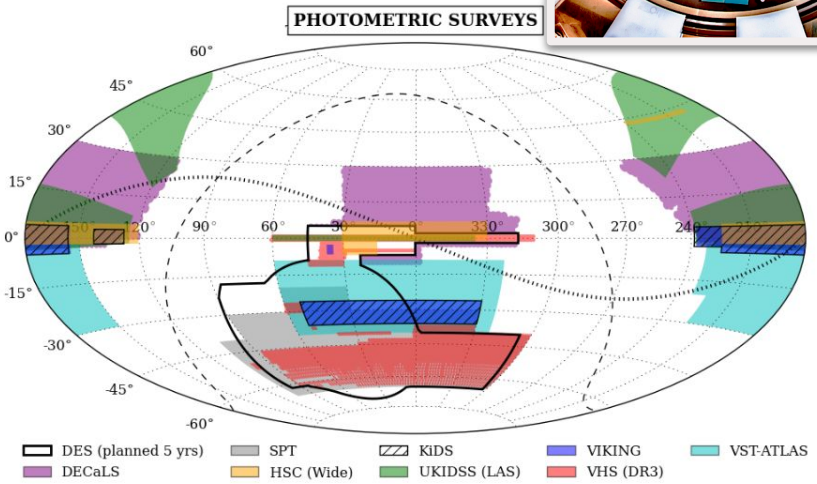

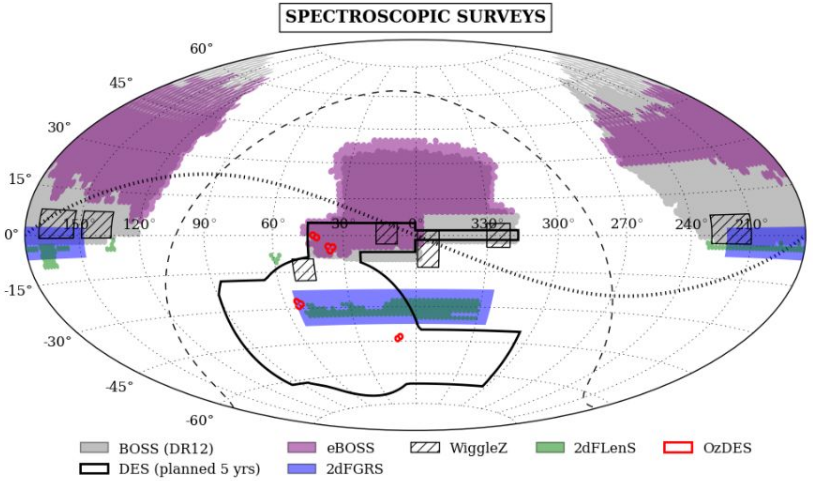

https://arxiv.org/abs/1601.00329

Cosmic probes within DES

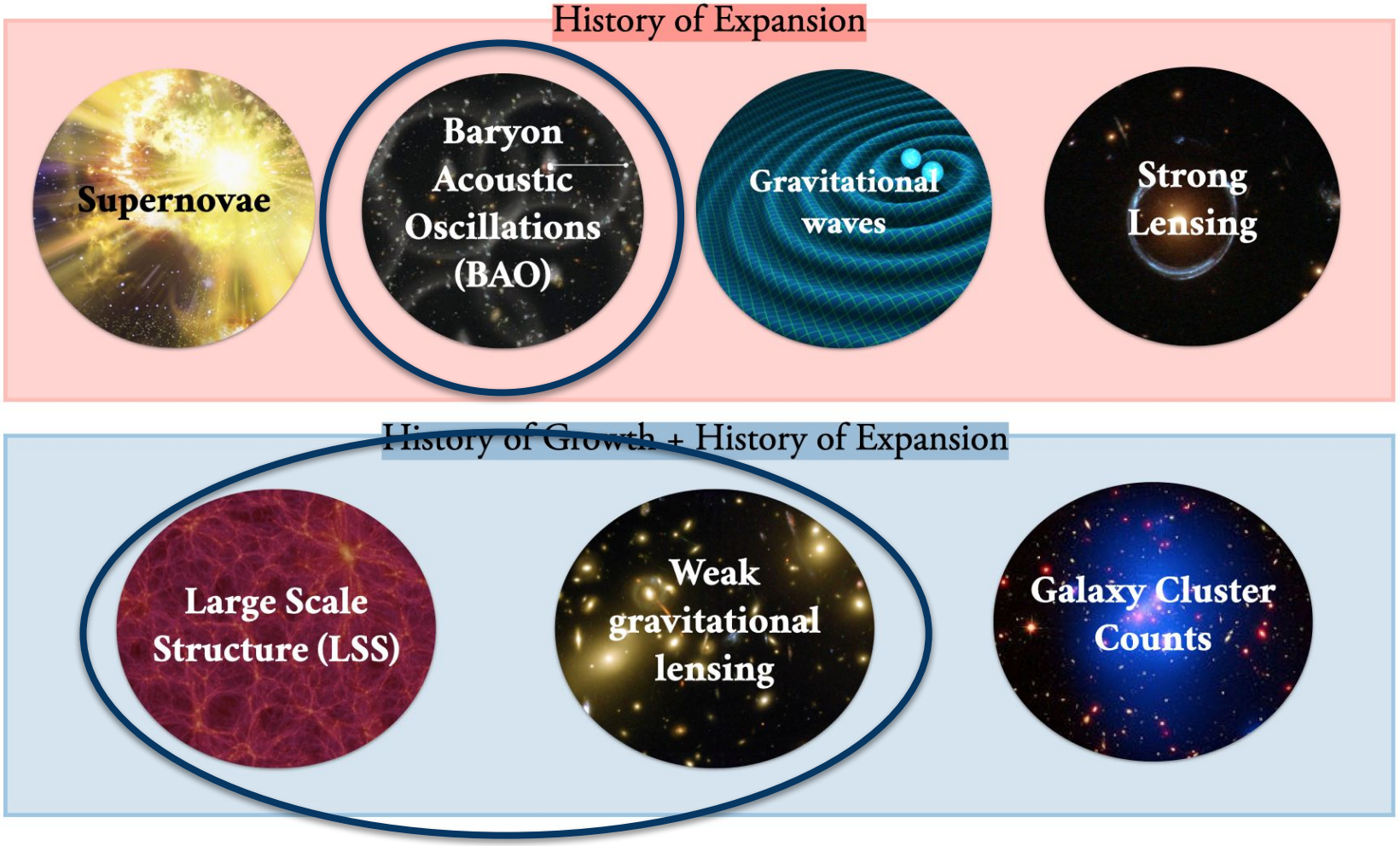

1) Cosmology from two-point correlations

Dark Energy Survey Year 3 results. List of key and supporting papers

1. "Blinding Multi-probe Cosmological Experiments" J. Muir, G. M. Bernstein, D. Huterer et al., arXiv: 1911.05929, MNRAS **494** (2020) 4454
2. "Photometric Data Set for Cosmology", I. Sevilla-Noarbe, K. Bechtol, M. Carrasco Kind et al., arXiv:2011.03407, ApJS **254** (2021) 24
3. "Weak Lensing Shape Catalogue", M. Gatti, E. Sheldon, A. Amon et al., arXiv:2011.03408, MNRAS **504** (2021) 4312
4. "Point Spread Function Modelling", M. Jarvis, G. M. Bernstein, A. Amon et al., arXiv:2011.03409, MNRAS **501** (2021) 1282
5. "Measuring the Survey Transfer Function with Balrog", S. Everett, B. Yanny, N. Kuropatkin et al., arXiv:2012.12825
6. "Deep Field Optical + Near-Infrared Images and Catalogue", W. Hartley, A. Choi, A. Amon et al., arXiv:2012.12824
7. "Blending Shear and Redshift Biases in Image Simulations", N. MacCrann, M. R. Becker, J. McCullough et al., arXiv:2012.08567
8. "Redshift Calibration of the Weak Lensing Source Galaxies", J. Myles, A. Alarcon, A. Amon et al., arXiv:2012.08566
9. "Redshift Calibration of the MagLim Lens Sample using Self-Organizing Maps and Clustering Redshifts", G. Giannini et al., in prep.
10. "Clustering Redshifts – Calibration of the Weak Lensing Source Redshift Distributions with redMaGiC and BOSS/eBOSS", M. Gatti, G. Giannini, et al., arXiv:2012.08569
11. "Calibration of Lens Sample Redshift Distributions using Clustering Redshifts with BOSS/eBOSS", R. Cawthon et al. arXiv:2012.12826
12. "Phenotypic Redshifts with SOMs: a Novel Method to Characterize Redshift Distributions of Source Galaxies for Weak Lensing Analysis" R. Buchs, C.Davis, D. Gruen et al. arXiv:1901.05005, MNRAS **489** (2019) 820
13. "Marginalising over Redshift Distribution Uncertainty in Weak Lensing Experiments", J. Cordero, I. Harrison et al., in prep.
14. "Exploiting Small-Scale Information using Lensing Ratios", C. Sánchez, J. Prat et al., in prep.
15. "Cosmology from Combined Galaxy Clustering and Lensing - Validation on Cosmological Simulations", J. de Rose et al., in prep.
16. "Unbiased fast sampling of cosmological posterior distributions", P. Lemos, R. Rollins, N. Weaverdyck, A. Ferte, A. Liddle et al., in prep.
17. "Assessing Tension Metrics with DES and Planck Data", P. Lemos, M. Raveri, A. Campos et al., arXiv:2012.09554
18. "Dark Energy Survey Internal Consistency Tests of the Joint Cosmological Probe Analysis with Posterior Predictive Distributions", C. Doux, E. Baxter, P. Lemos et al. arXiv:2011.03410, MNRAS **503** (2021) 2688
19. "Covariance Modelling and its Impact on Parameter Estimation and Quality of Fit", O. Friedrich, F. Andrade-Oliveira, H. Camacho et al., arXiv:2012.08568
20. "Multi-Probe Modeling Strategy and Validation", E. Krause et al., in prep.
21. "Curved-Sky Weak Lensing Map Reconstruction", N. Jeffrey, M. Gatti, C. Chang et al., in prep.
22. "Galaxy Clustering and Systematics Treatment for Lens Galaxy Samples", M.Rodríguez-Monroy, N. Weaverdyck, J. Elvin-Poole, M. Crocce et al., in prep.
23. "Optimizing the Lens Sample in Combined Galaxy Clustering and Galaxy-Galaxy Lensing Analysis", A. Porredon, M. Crocce et al., arXiv:2011.03411 PhRvD **103** (2021) 043503
24. "High-Precision Measurement and Modeling of Galaxy-Galaxy Lensing", J. Prat, J. Blazek, C. Sánchez et al., in prep.
25. "Constraints on Cosmological Parameters and Galaxy Bias Models from Galaxy Clustering and Galaxy-Galaxy Lensing using the redMaGiC Sample", S. Pandey et al., in prep.
26. "Cosmological Constraints from Galaxy Clustering and Galaxy-Galaxy Lensing using the Maglim Lens Sample" A. Porredon, M. Crocce et al., in prep.
27. "Cosmology from Cosmic Shear and Robustness to Data Calibration", A. Amon, D. Gruen, M. A. Troxel et al., in prep.
28. "Cosmology from Cosmic Shear and Robustness to Modeling Assumptions", L. Secco, S. Samuroff et al., in prep.
29. "Magnification modeling and impact on cosmological constraints from galaxy clustering and galaxy-galaxy lensing", J. Elvin-Poole, N. MacCrann et al., in prep.
30. "Cosmological Constraints from Galaxy Clustering and Weak Lensing" The DES Collaboration in prep.

Observing the large scale structure

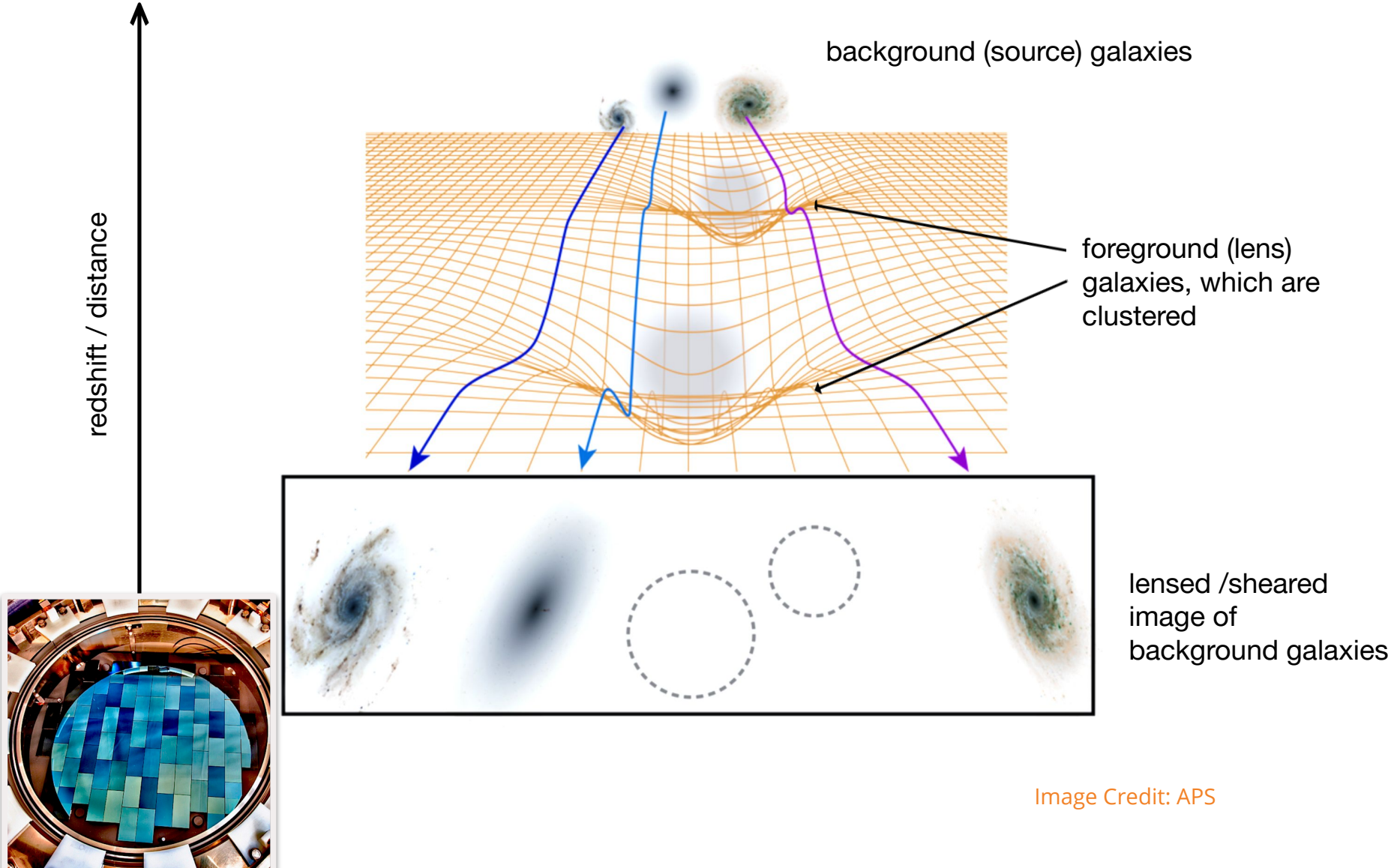

Image Credit: APS

Weak lensing

When light passes through foreground structures, gravity imprints coherent distortions:

This causes shifting, and magnification, and shearing of background galaxy images.

We measure the correlation of the **shapes** of source galaxy pairs as a function of angular radius and in source **redshift** bins or tomographically.

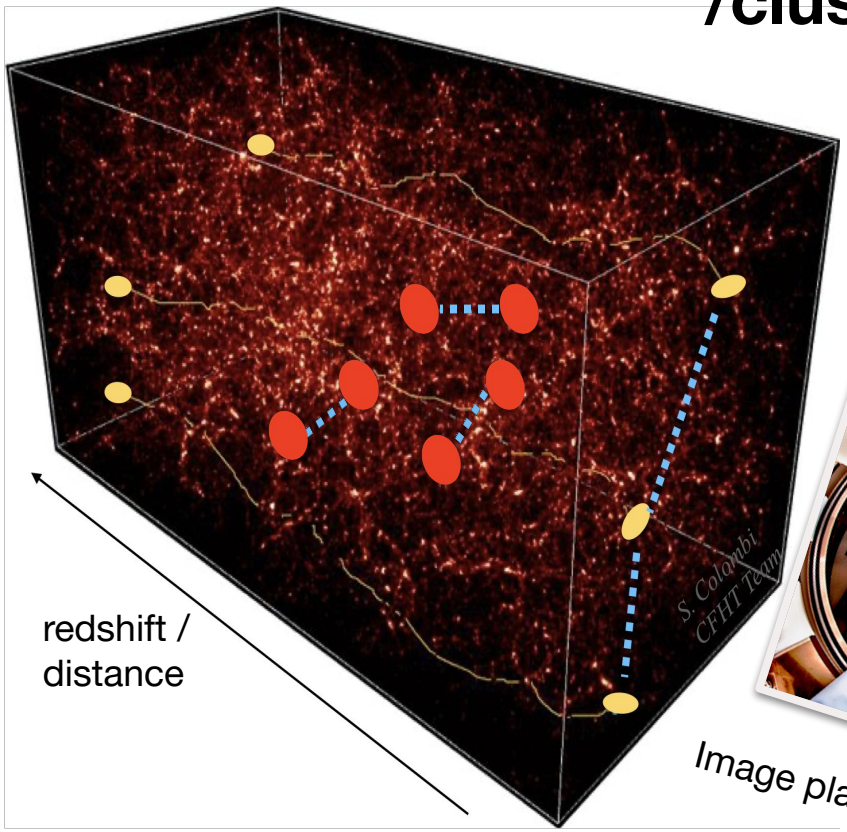

Galaxy distribution /clustering

Galaxies trace the underlying dark matter structure: they are observed to be spatially *clustered*.

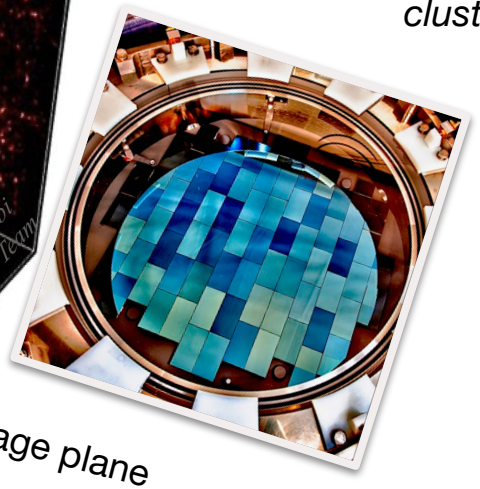

Need to measure **galaxy shapes**, **positions** and **redshift distributions**

Image Credit: S. Colombi / IAP

Clustering: Two-point correlation function interpretation

$$\langle \mathrm{d}N_{\mathrm{pairs}}(r,\hat{\mathbf{n}})\rangle = \bar{n}_{\mathrm{g}}^2\,[1+\langle \delta_{\mathrm{g}}(\mathbf{x})\delta_{\mathrm{g}}(\mathbf{x}+r\hat{\mathbf{n}})\rangle]\,\mathrm{d}V_1\,\mathrm{d}V_2$$

Two point correlation function:

$$\xi_{\mathrm{g}}(r,\hat{\mathbf{n}}) = \langle \delta_{\mathrm{g}}(\mathbf{x})\delta_{\mathrm{g}}(\mathbf{x}+r\hat{\mathbf{n}})\rangle$$

- Contain information about the scale of BAO!

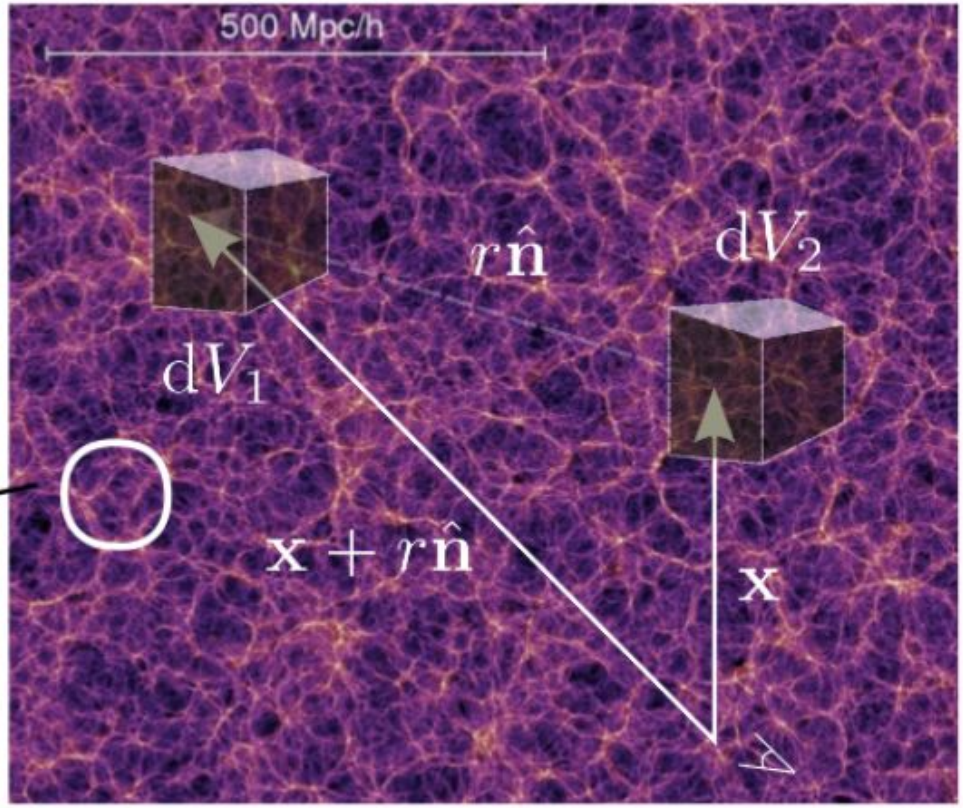

Excess of probability wrt a random distribution for finding pairs of tracers separated by a given distance

3x2pt cosmology

A self-consistent combined analysis maximises the cosmological information and robustly constrains astrophysical & observational systematic priors in the analysis!

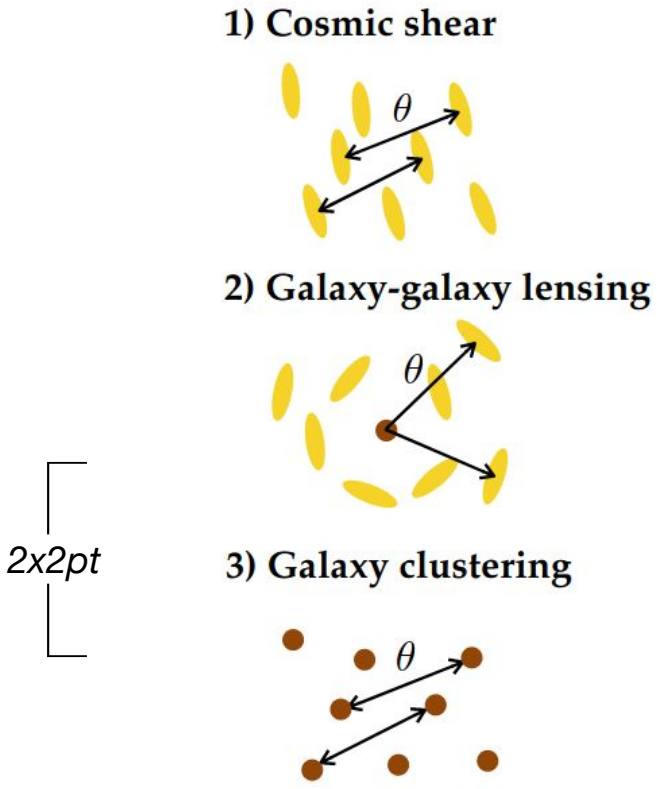

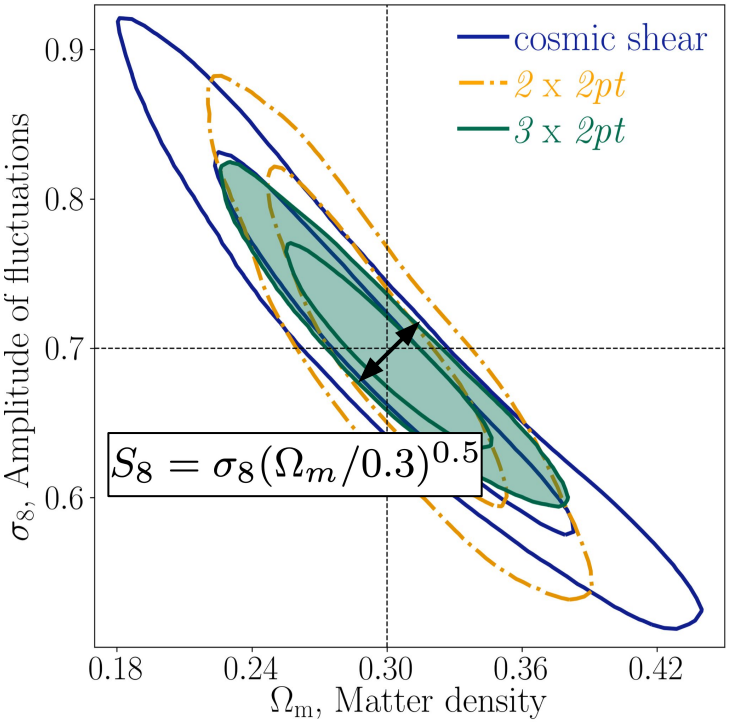

Image credit: Chihway Chang

Galaxy shapes measurement: *Metacalibration*

$$\hat{\vec{\gamma}}_i = \langle R_i \rangle^{-1} \vec{e}_i,$$

Measure **response** on ellipticity estimator to artificially-applied shear (Huff & Mandelbaum 2017, Sheldon & Huff 2017)

Unbiased in limit of:

- weak shear
- isolated galaxy images
- perfect knowledge of PSF

Use **simulations to calibrate bias** from, e.g., **blending** of galaxy images

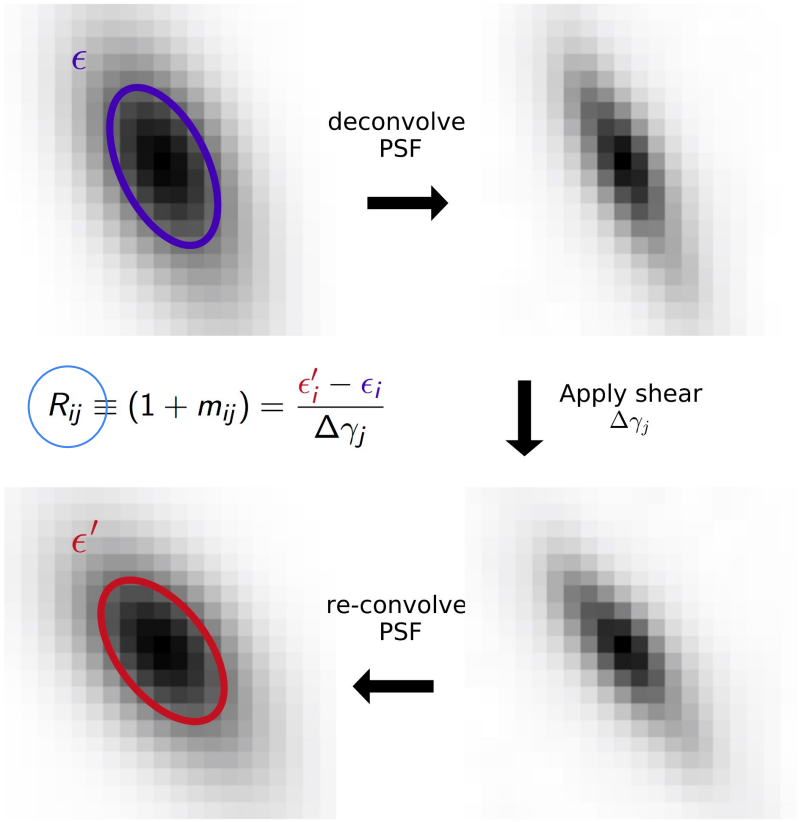

Image credit: **Niall MacCrann**

(Jarvis+2021) (**Gatti**,Sheldon+2021) (**MacCrann**+2021)

Galaxy shapes catalog

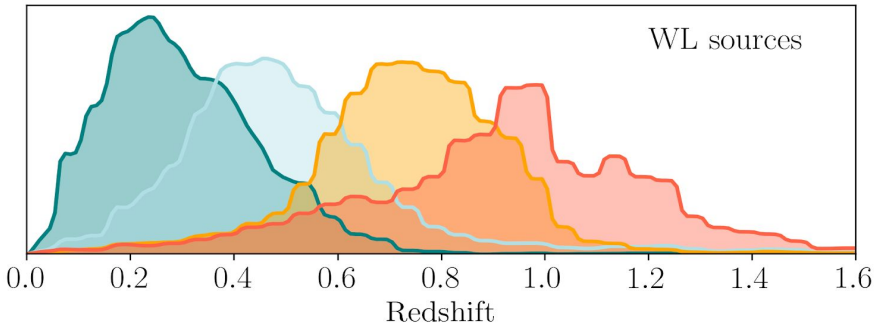

# galaxies	n_{eff} [gal/sq.arcmin]	σ_e
100 204 026	5.590	0.268

cf. DES SV: 2-3 million shapes
DES Y1: 34.8 million

Key improvements over DES Y1:

- Redshift distributions from at least two independent methods:
  - Photometry (colors) SOMPZ
    Myles, Alarcon et al. (2021)
  - Lensing (shapes): Shear Ratio (SR)
    Sánchez, Prat, et al. (2021)
- More accurate **PSF modeling**
  (Jarvis+2021)
- Improved astrometry
- Expanded suite of **null tests**
  (**Gatti**,Sheldon+2021)
- Calibration using realistic image sims that characterize the **impact of blending** on both shear and redshifts
  (**MacCrann**+2021)

"With great statistical power comes great systematic responsibility"

Cosmic shear measurements: shape-shape correlations

S/N ~27 (Y1) → 40 (Y3)

Correlation of shapes of galaxy pairs

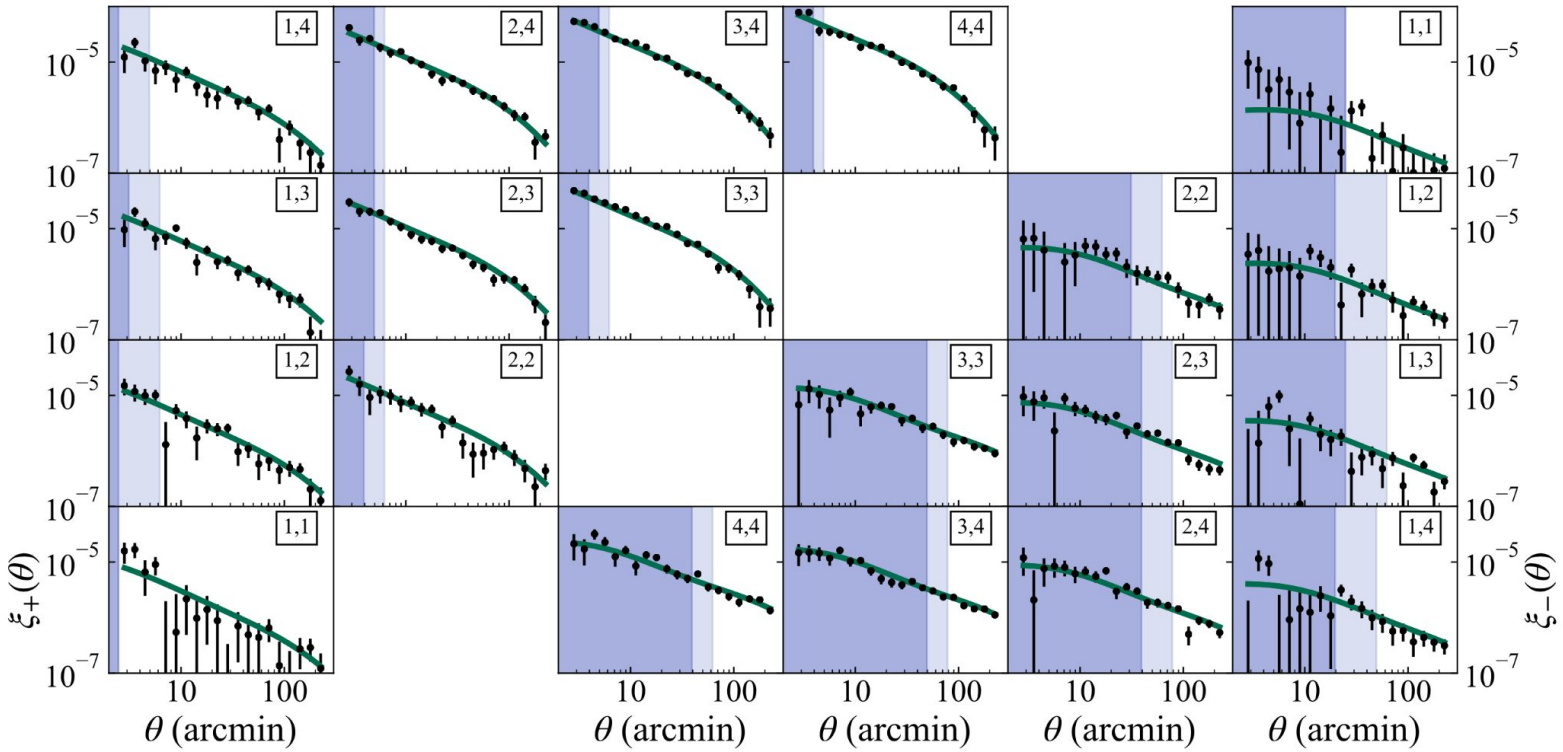

Amon+2021 Secco, Samuroff+2021

Galaxy clustering: two foreground (lens) samples

redMaGiC

- LRG selection also used in Y1 analysis
- *p(z)*s are stacked, and then validated using clustering redshifts **Cawthon** et al. (2021)

MagLim **Porredon,** et al. (2020)

- Bright selection -> higher z
- Defined using machine-learning photometric redshifts (DNF **de Vicente** et al (2015)), and also validated using WZ **Cawthon** et al. (2021)
- Additional validation using SOMPZ **Giannini** et al. (in prep)

Shear Ratios were also used for validation in all cases **Sánchez, Prat,** et al. (2021).

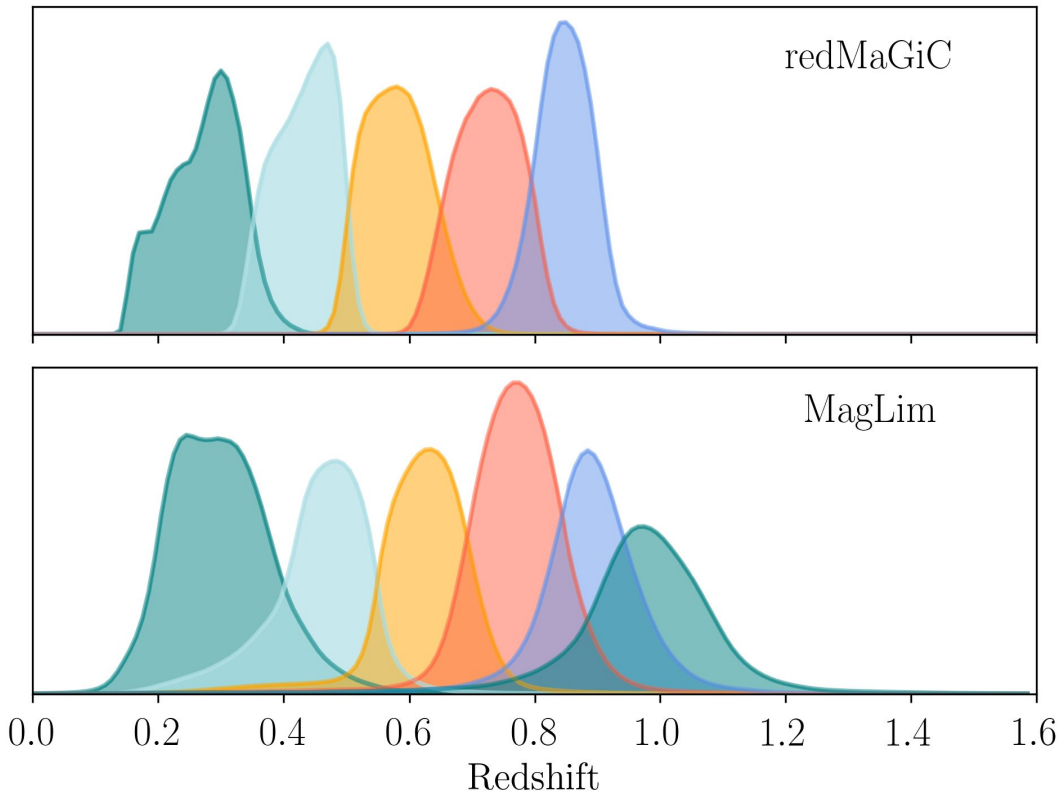

LSS systematics

Mitigation of correlation with survey properties and astrophysical maps is done by re-weighting galaxy sample by fitted relation

Accounts for correlation with:
airmass, seeing, exposure time, depth, stellar density, dust, sky brightness, calibration residuals

Correct with two template based methods:

- **Iterative systematics decontamination (ISD)** (**Elvin-Poole** et al 2017 **Rodriguez-Monroy** et al 2021)
- **Elastic Net (ENET)** (**Weaverdyck** et al 2020)

Analytically marginalize over difference in methods and bias from simulations

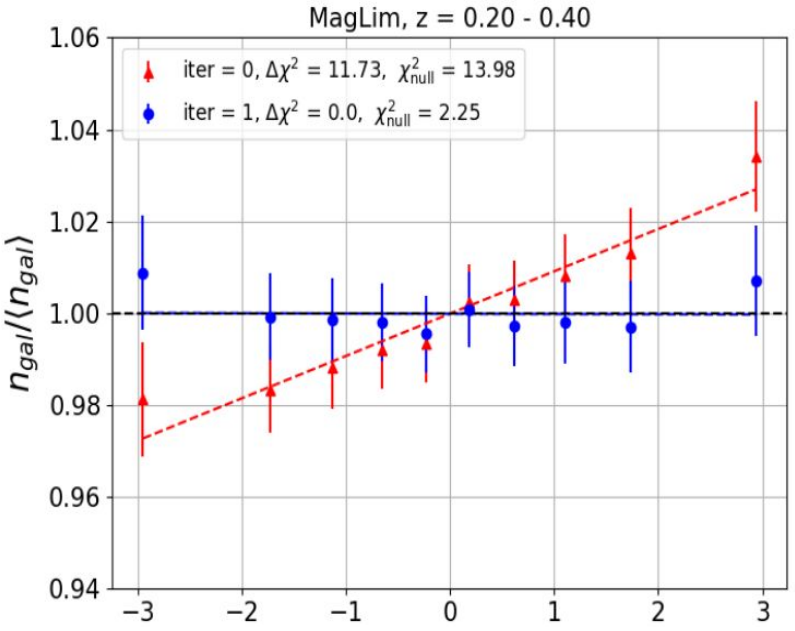

Linear combination of survey maps

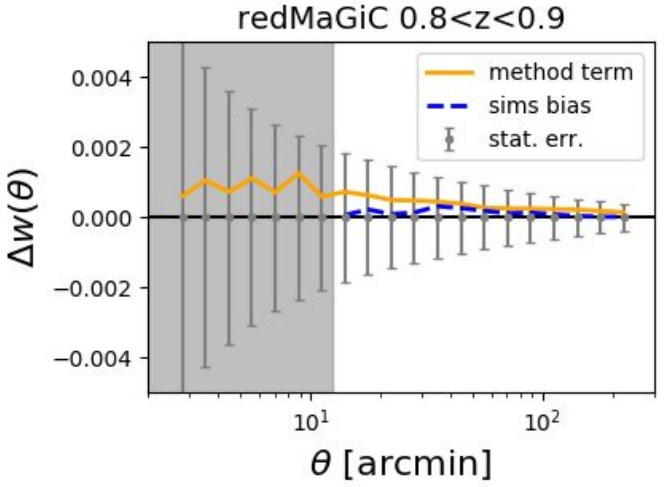

Rodriguez-Monroy et al. (2021)

"With great statistical power comes great systematic responsibility"

LSS systematics

Mitigation of correlation with survey properties and astrophysical maps is done by re-weighting galaxy sample by fitted relation

Accounts for correlation with:
airmass, seeing, exposure time, depth, stellar density, dust, sky brightness, calibration residuals

Correct with two template based methods:

- **Iterative systematics decontamination (ISD)** (**Elvin-Poole** et al 2017 **Rodriguez-Monroy** et al 2021)
- **Elastic Net (ENET)** (**Weaverdyck** et al 2020)

Analytically marginalize over difference in methods and bias from simulations

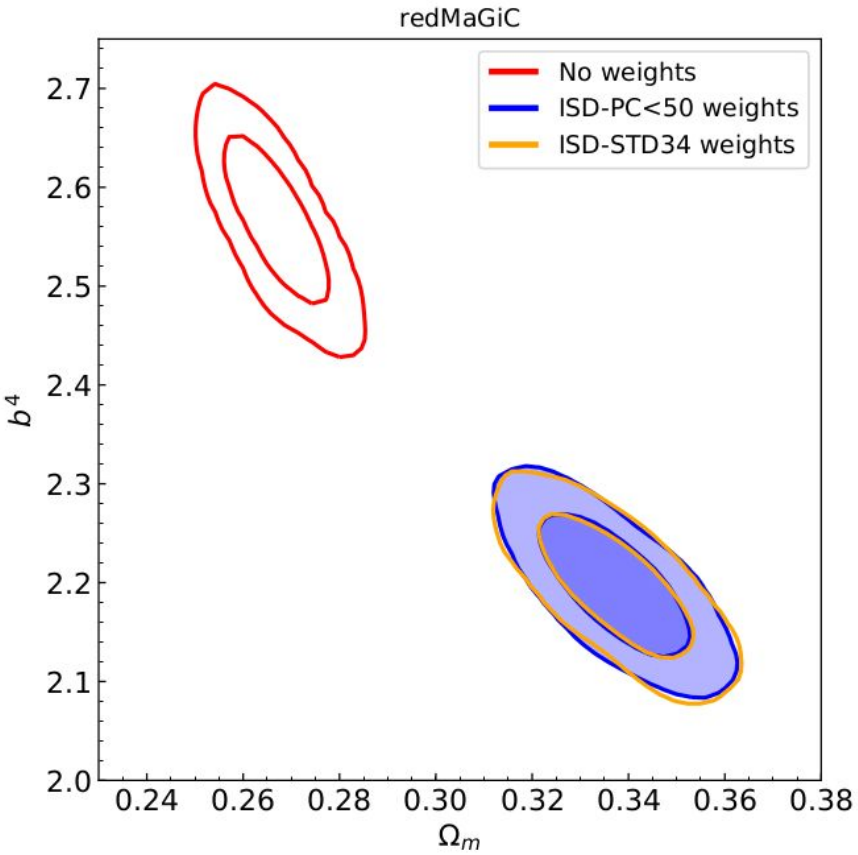

"With great statistical power comes great systematic responsibility"

Rodriguez-Monroy et al. (2021)

Galaxy Clustering: measurements of position position correlations

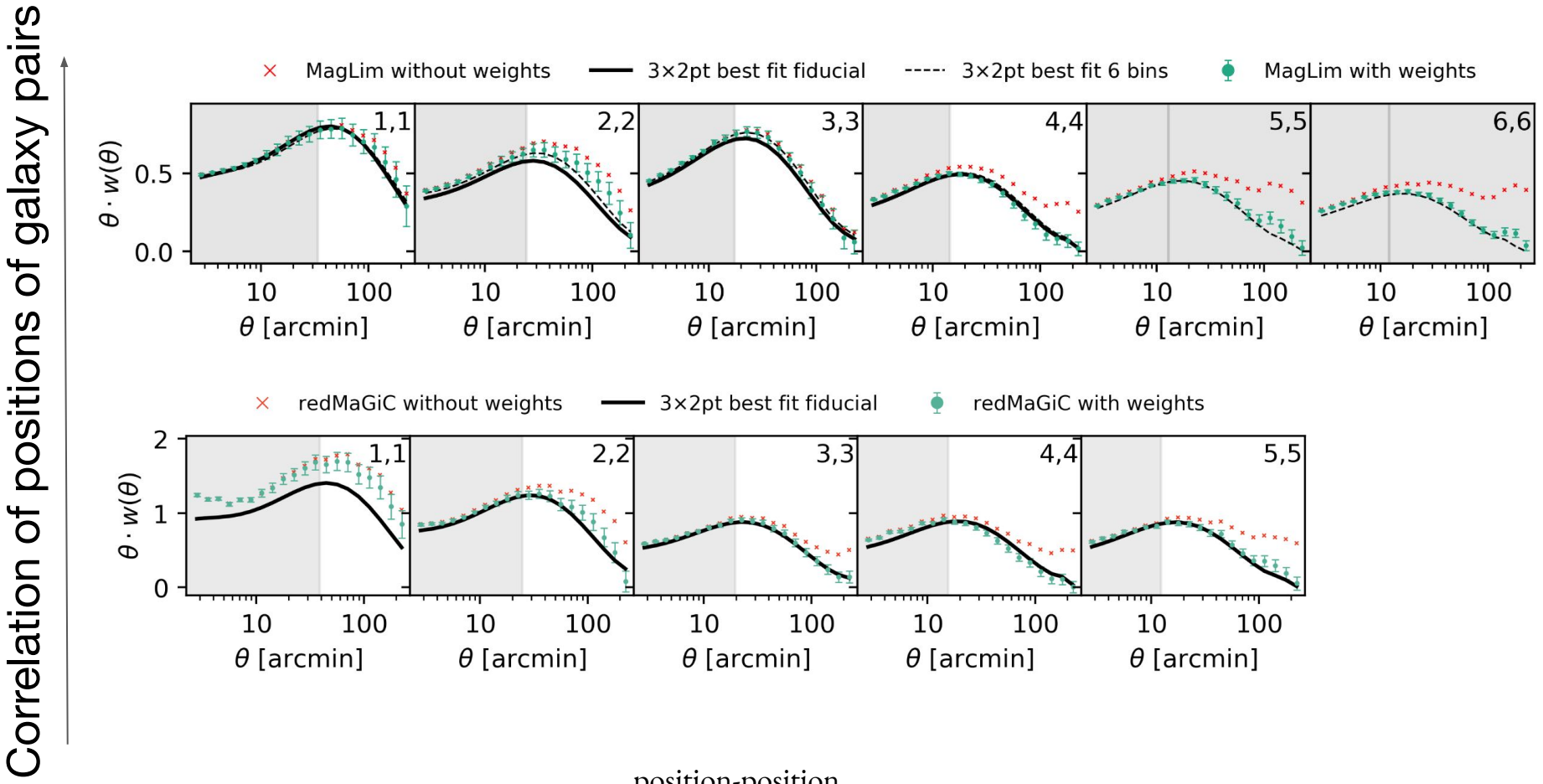

position-position

Rodriguez-Monroy et al. (2021)

Galaxy-Galaxy lensing measurements

position-shape

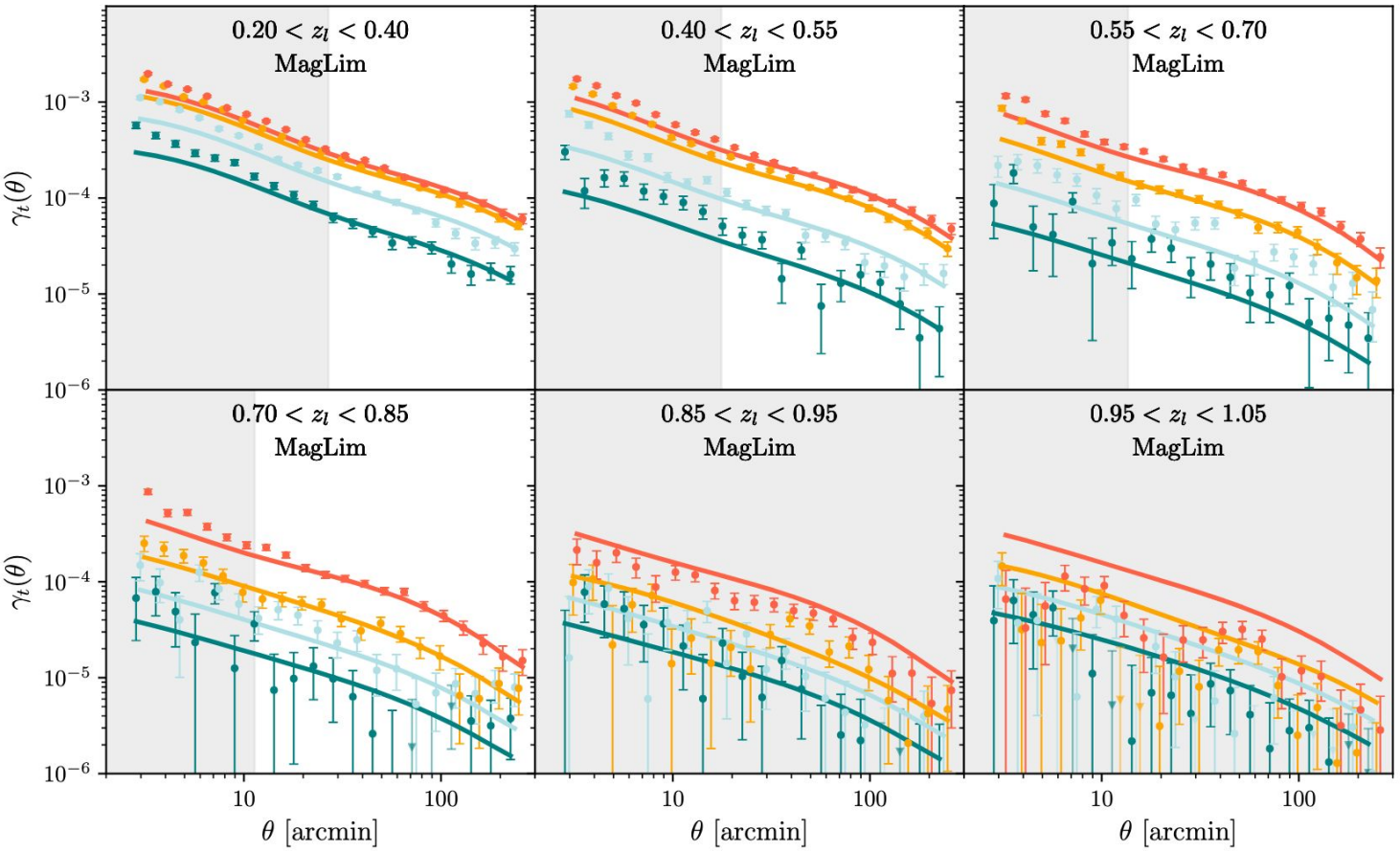

Measured on both lens samples

Used to construct shear ratios **Sánchez, Prat,** et al. (2021)

- Additional redshift method
- Weak dependence on the galaxy-matter power spectrum -> smaller scales.

Prat et al (2021)

From 3x2pt Measurements to Cosmology Constraints

Infer parameter posterior $P(\mathbf{p}|\hat{\mathbf{D}}, M)$ within model M using Bayes' theorem

$$P(\mathbf{p}|\hat{\mathbf{D}}, M) \propto \mathcal{L}(\hat{\mathbf{D}}|\mathbf{p}, M) P(\mathbf{p}|M)$$

Required Ingredients

- Data likelihood $\mathcal{L}(\hat{\mathbf{D}}|\mathbf{p}, M)$ with data covariance **C**
- Model M with parameters **p**, and prior, $P(\mathbf{p}|M)$
- Criteria which measurements to combine
- Blinding scheme to minimize observer bias

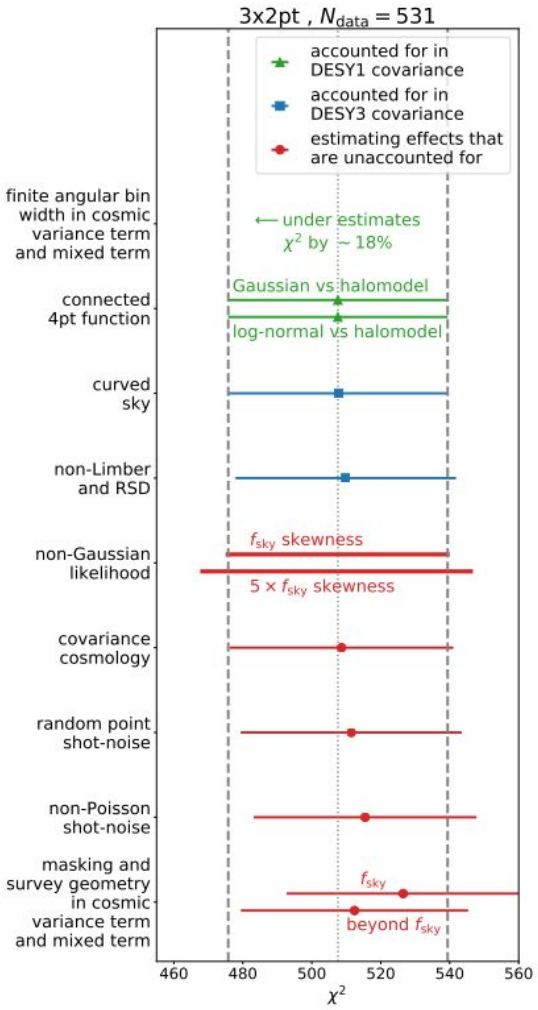

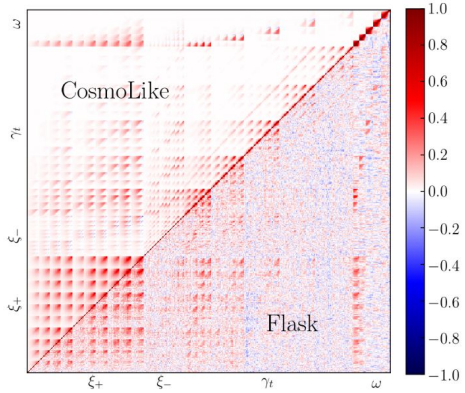

Friedrich, Andrade-Oliveira, Camacho et. al. (2021)

From 3x2pt Measurements to Cosmology Constraints

Infer parameter posterior $P(\mathbf{p}|\hat{\mathbf{D}}, M)$ within model M using Bayes' theorem

$$P(\mathbf{p}|\hat{\mathbf{D}}, M) \propto \mathcal{L}(\hat{\mathbf{D}}|\mathbf{p}, M)P(\mathbf{p}|M)$$

Required Ingredients

- Data likelihood $\mathcal{L}(\hat{\mathbf{D}}|\mathbf{p}, M)$ with data covariance **C**
- Model M with parameters **p**, and prior, $P(\mathbf{p}|M)$
- Criteria which measurements to combine
- Blinding scheme to minimize observer bias

Parameter		Prior
Cosmology		
$\Omega_{\rm m}$	Flat	(0.1, 0.9)
$10^9 A_{\rm s}$	Flat	(0.5, 5.0)
$n_{\rm s}$	Flat	(0.87, 1.07)
$\Omega_{\rm b}$	Flat	(0.03, 0.07)
h	Flat	(0.55, 0.91)
$10^3 \Omega_\nu h^2$	Flat	(0.60, 6.44)
w	Flat	$(-2.0, -0.33)$
Lens Galaxy Bias		
$b_i (i \in [1, 4])$	Flat	(0.8, 3.0)
Lens magnification		
$C_{\rm l}^1$	Fixed	1.21
$C_{\rm l}^2$	Fixed	1.15
$C_{\rm l}^3$	Fixed	1.88
$C_{\rm l}^4$	Fixed	1.97
Lens photo-z		
$\Delta z_{\rm l}^1 \times 10^2$	Gaussian	$(-0.9, 0.7)$
$\Delta z_{\rm l}^2 \times 10^2$	Gaussian	$(-3.5, 1.1)$
$\Delta z_{\rm l}^3 \times 10^2$	Gaussian	$(-0.5, 0.6)$
$\Delta z_{\rm l}^4 \times 10^2$	Gaussian	$(-0.7, 0.6)$
$\sigma_{z,{\rm l}}^1$	Gaussian	(0.98, 0.06)
$\sigma_{z,{\rm l}}^2$	Gaussian	(1.31, 0.09)
$\sigma_{z,{\rm l}}^3$	Gaussian	(0.87, 0.05)
$\sigma_{z,{\rm l}}^4$	Gaussian	(0.92, 0.05)
Intrinsic Alignment		
a_i $(i \in [1, 2])$	Flat	$(-5, 5)$
η_i $(i \in [1, 2])$	Flat	$(-5, 5)$
$b_{\rm TA}$	Flat	$(0, 2)$
z_0	Fixed	0.62
Source photo-z		
$\Delta z_{\rm s}^1 \times 10^2$	Gaussian	(0.0, 1.8)
$\Delta z_{\rm s}^2 \times 10^2$	Gaussian	(0.0, 1.5)
$\Delta z_{\rm s}^3 \times 10^2$	Gaussian	(0.0, 1.1)
$\Delta z_{\rm s}^4 \times 10^2$	Gaussian	(0.0, 1.7)
Shear calibration		
$m^1 \times 10^2$	Gaussian	$(-0.6, 0.9)$
$m^2 \times 10^2$	Gaussian	$(-2.0, 0.8)$
$m^3 \times 10^2$	Gaussian	$(-2.4, 0.8)$
$m^4 \times 10^2$	Gaussian	$(-3.7, 0.8)$

Krause et al (2021)

From 3x2pt Measurements to Cosmology Constraints

Infer parameter posterior $P(\mathbf{p}|\hat{\mathbf{D}}, M)$ within model M using Bayes' theorem

$$P(\mathbf{p}|\hat{\mathbf{D}}, M) \propto \mathcal{L}(\hat{\mathbf{D}}|\mathbf{p}, M)P(\mathbf{p}|M)$$

Required Ingredients

- Data likelihood $\mathcal{L}(\hat{\mathbf{D}}|\mathbf{p}, M)$ with data covariance **C**
- Model M with parameters **p**, and prior, $P(\mathbf{p}|M)$
- Criteria for scales to consider.
- Criteria which measurements to combine
- Blinding scheme to minimize observer bias

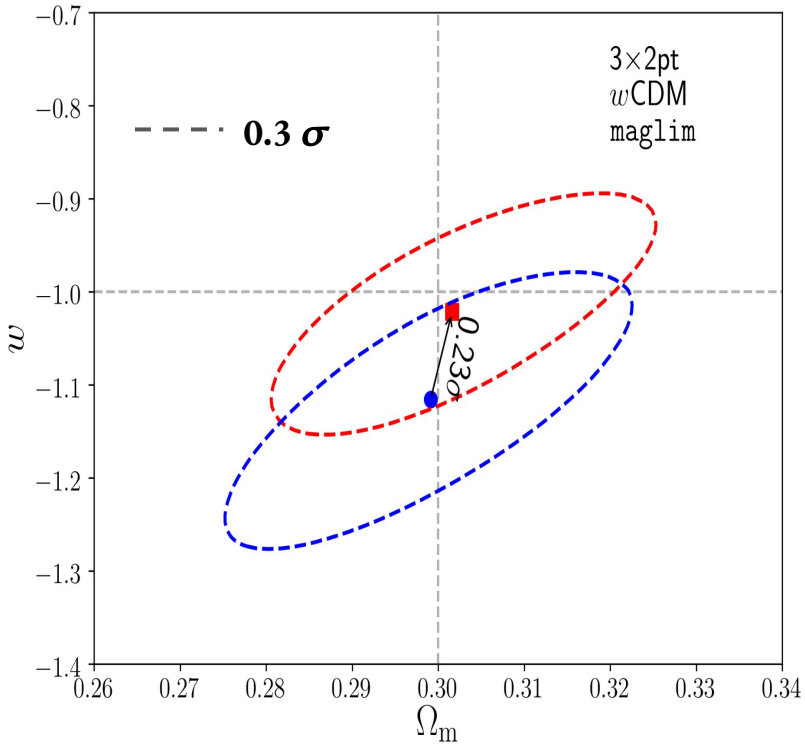

Krause et. al. (2021)

De Rose et. al. (2021)

From 3x2pt Measurements to Cosmology Constraints

Infer parameter posterior $P(\mathbf{p}|\hat{\mathbf{D}}, M)$ within model M using Bayes' theorem

$$P(\mathbf{p}|\hat{\mathbf{D}}, M) \propto \mathcal{L}(\hat{\mathbf{D}}|\mathbf{p}, M) P(\mathbf{p}|M)$$

Required Ingredients

- Data likelihood $\mathcal{L}(\hat{\mathbf{D}}|\mathbf{p}, M)$ with data covariance **C**
- Model M with parameters **p**, and prior, $P(\mathbf{p}|M)$
- Criteria for scales to consider.
- Criteria which measurements to combine
- Blinding scheme to minimize observer bias (Muir+2020)

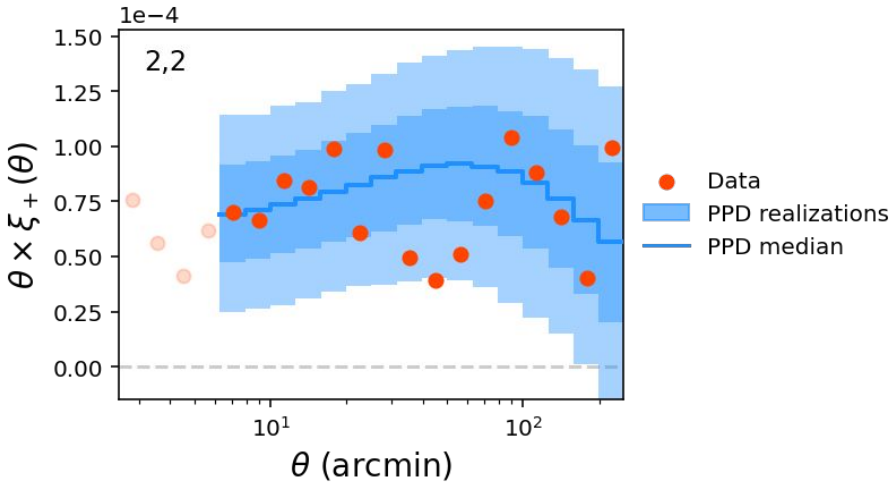

Internal consistency of 3x2pt data quantified in data space using Posterior Predictive Distribution (PPD)

Accept model fit if p>0.01

Doux, Baxter et. al. (2021)

DES Year 3 overview pipeline: pixels to cosmology

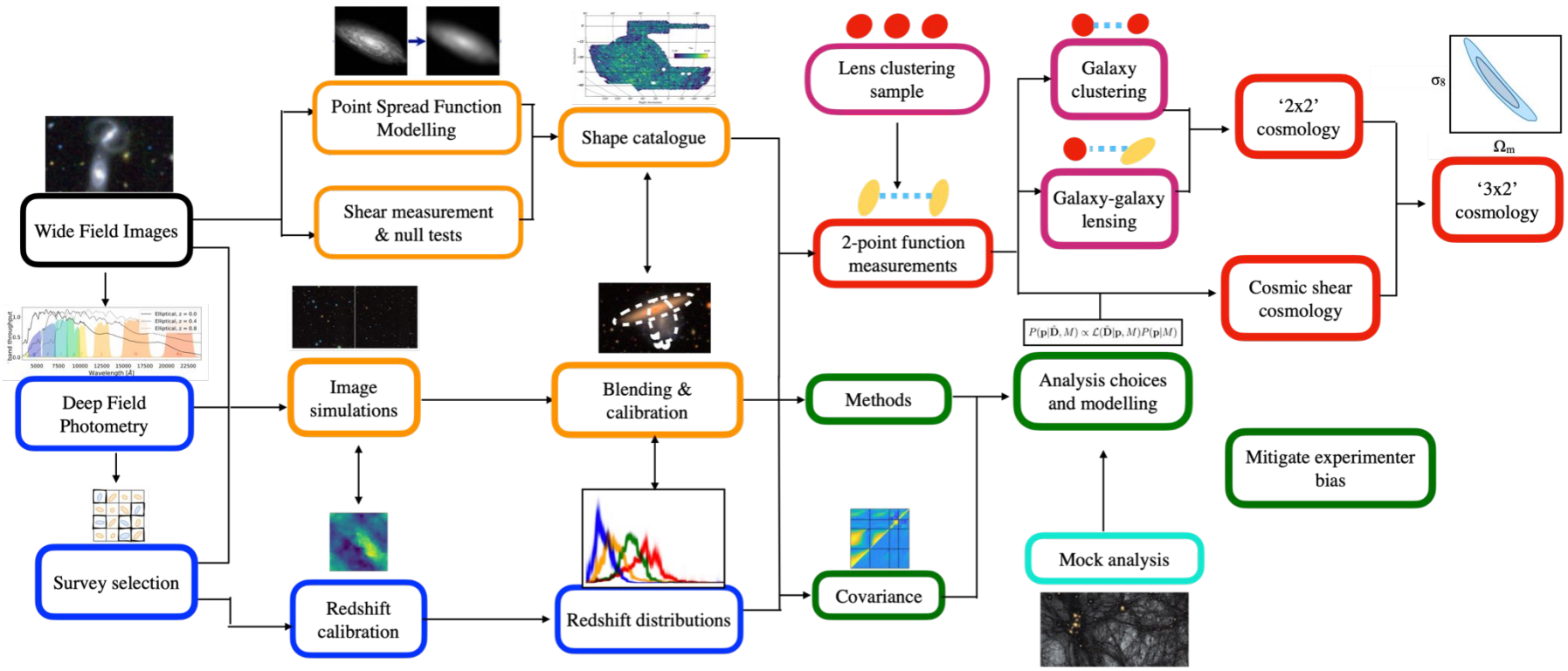

LCDM — WL+LSS — Redshifts — Shapes — Clustering — Simulations — Theory — Results

Key result: The DES 3x2pt constraints

- Cosmic shear most sensitive to clustering amplitude.
- Galaxy clustering and tangential shear more sensitive to total matter density.

A factor of 2.1 improvement in signal-to-noise from DES Year 1.

In ΛCDM:

$$S_8 = 0.776^{+0.017}_{-0.017} \quad (0.776)$$
$$\Omega_{\rm m} = 0.339^{+0.032}_{-0.031} \quad (0.372)$$
$$\sigma_8 = 0.733^{+0.039}_{-0.049} \quad (0.696)$$

In *w*CDM:

$$\Omega_{\rm m} = 0.352^{+0.035}_{-0.041} \quad (0.339)$$
$$w = -0.98^{+0.32}_{-0.20} \quad (-1.03)$$

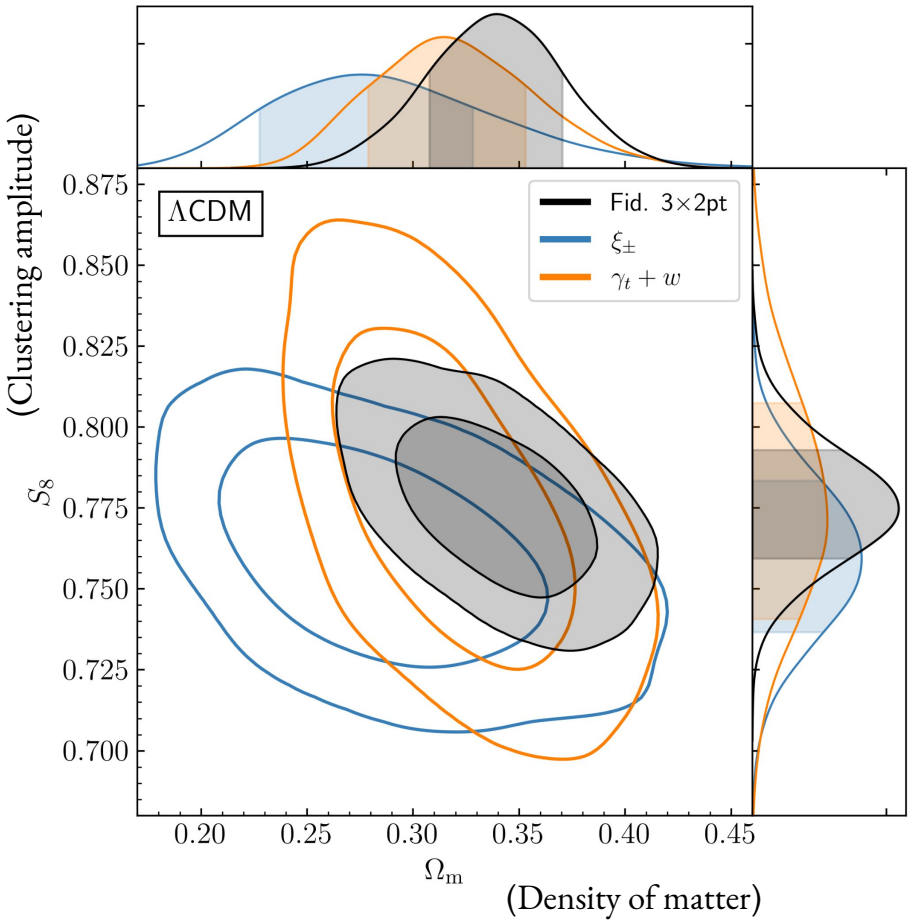

Lens sample comparison

Cosmic shear and galaxy clustering+tangential shear (2x2pt) for redMaGiC are also formally consistent and combine to give the **3x2pt** result.

2x2pt prefers lower S8 and higher galaxy bias. Combination with cosmic shear brings S8 up and bias down to agree with DES Y1.

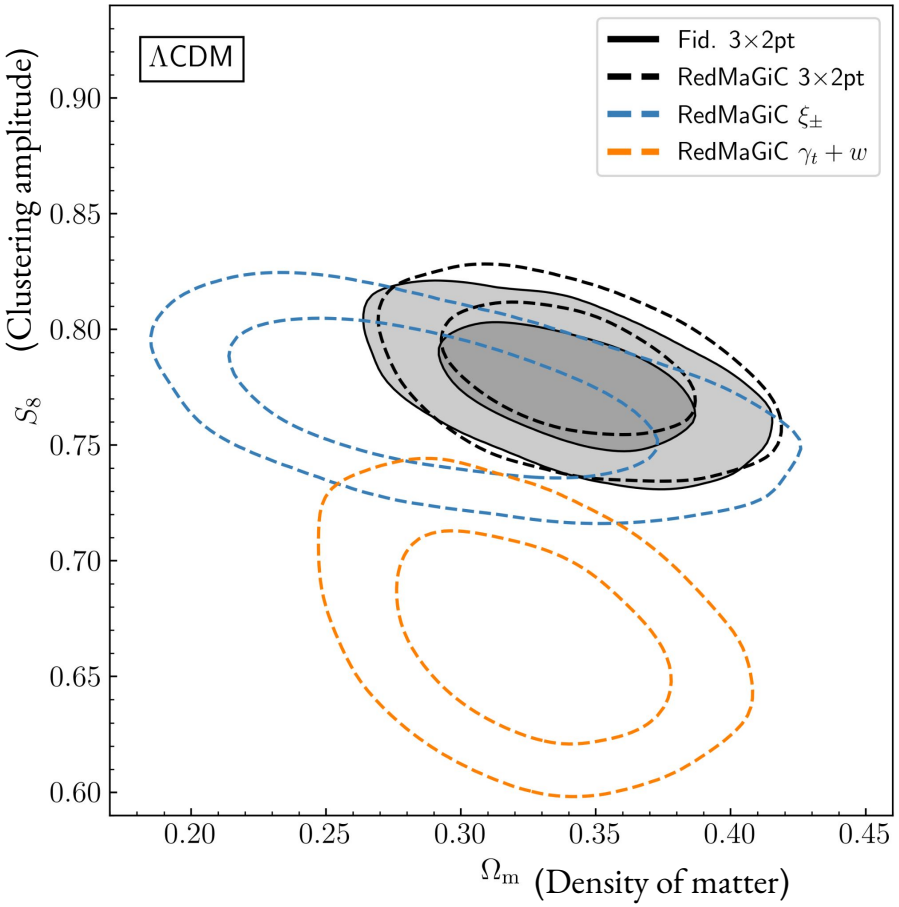

Lens sample comparison

We introduce a parameter X_{lens} to model this, which decorrelates the clustering and lensing amplitudes:

$$w^{ii}(\theta) = b_i^2 \xi^{ii}_{\rm mm}(\theta)$$
$$\gamma_t^{ij}(\theta) = X_{\rm lens} b_i \xi^{ij}_{\rm mm}(\theta)$$

$$X_{\rm lens} = 0.877^{+0.026}_{-0.019}$$

X_{lens} does not strongly impact ΛCDM results, but is highly correlated with *w* in redMaGiC *w*CDM.

- **What is X_{lens}?**

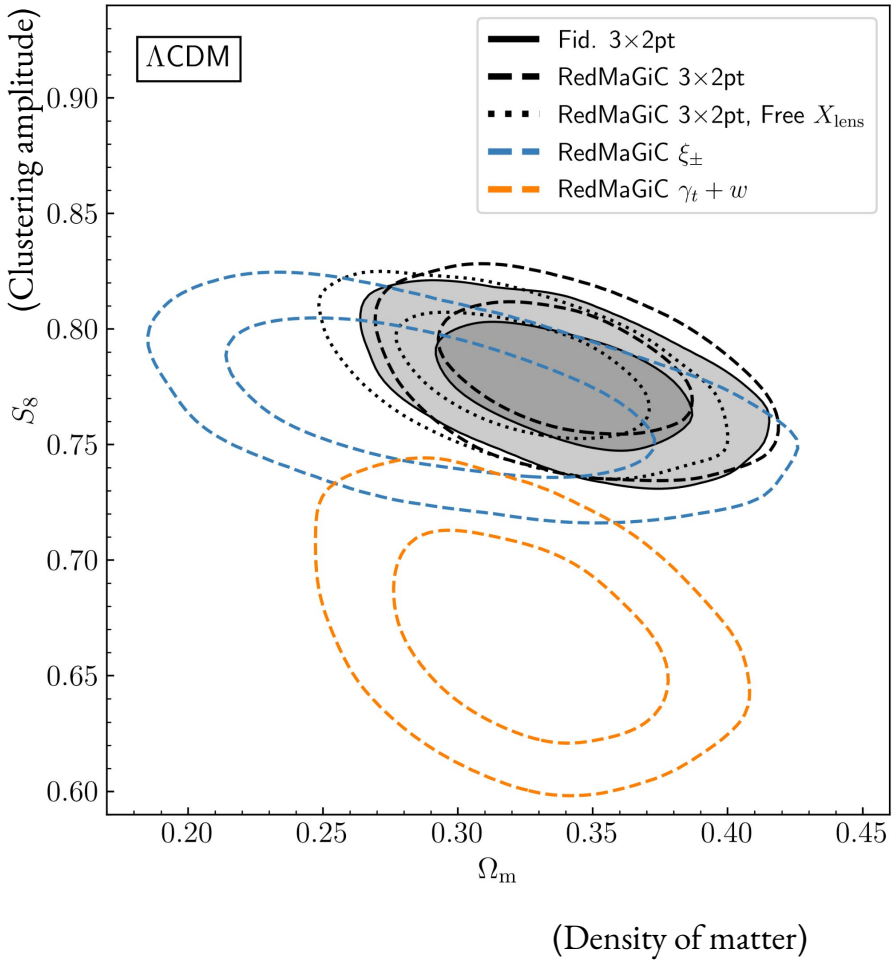

Low-z vs High-z in ΛCDM

Similar constraints between **DES Y3 3x2pt** and *Planck* CMB for the clustering amplitude. Planck does better for the density of matter.

No evidence of inconsistency: 0.7-1.5σ or p=0.13-0.48.

Combining is possible and improves the clustering amplitude

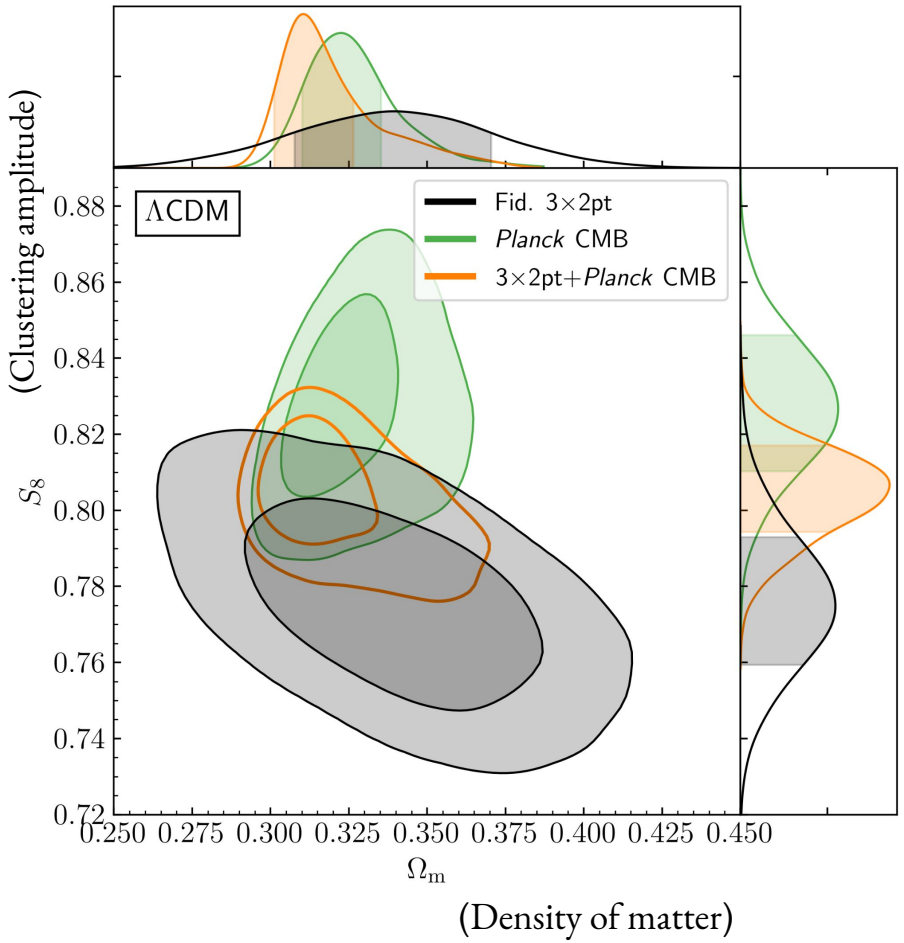

Key result: Consistency and combination with external low-z (SNe Ia, BAO, RSD)

All consistent within 1σ.

Combination of DES and the other complementary low-redshift probes results consistent with Planck CMB at 0.9σ or p=0.34.

External low-z and DES are highly complementary.

All low-z gives competitive constraints compared to Planck CMB

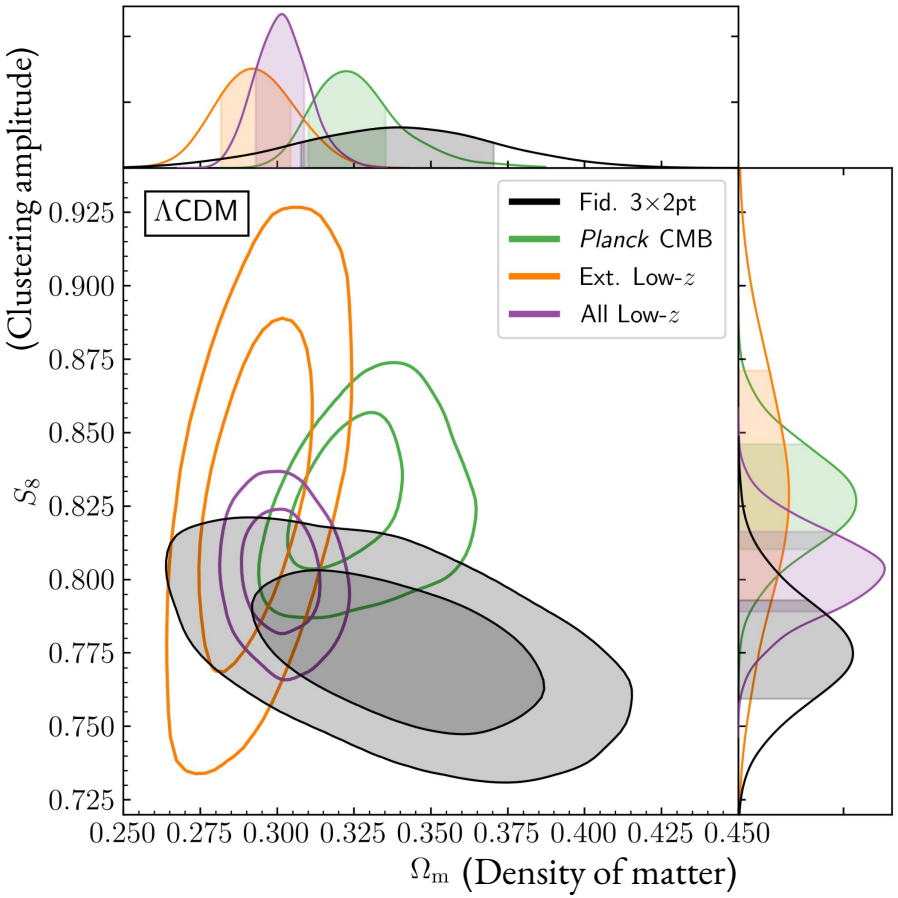

Key result: DES + External low z (SNe Ia, BAO, RSD) + CMB - tightest constraints

In ΛCDM:

$$S_8 = 0.812^{+0.008}_{-0.008} \quad (0.815)$$

$$\Omega_{\rm m} = 0.306^{+0.004}_{-0.005} \quad (0.306)$$

$$\sigma_8 = 0.804^{+0.008}_{-0.008} \quad (0.807)$$

$$h = 0.680^{+0.004}_{-0.003} \quad (0.681)$$

$$\sum m_\nu < 0.13 \text{ eV } (95\% \text{ CL})$$

In *w*CDM:

$$\sigma_8 = 0.810^{+0.010}_{-0.009} \quad (0.804),$$

$$\Omega_{\rm m} = 0.302^{+0.006}_{-0.006} \quad (0.298),$$

$$w = -1.03^{+0.03}_{-0.03} \quad (-1.00)$$

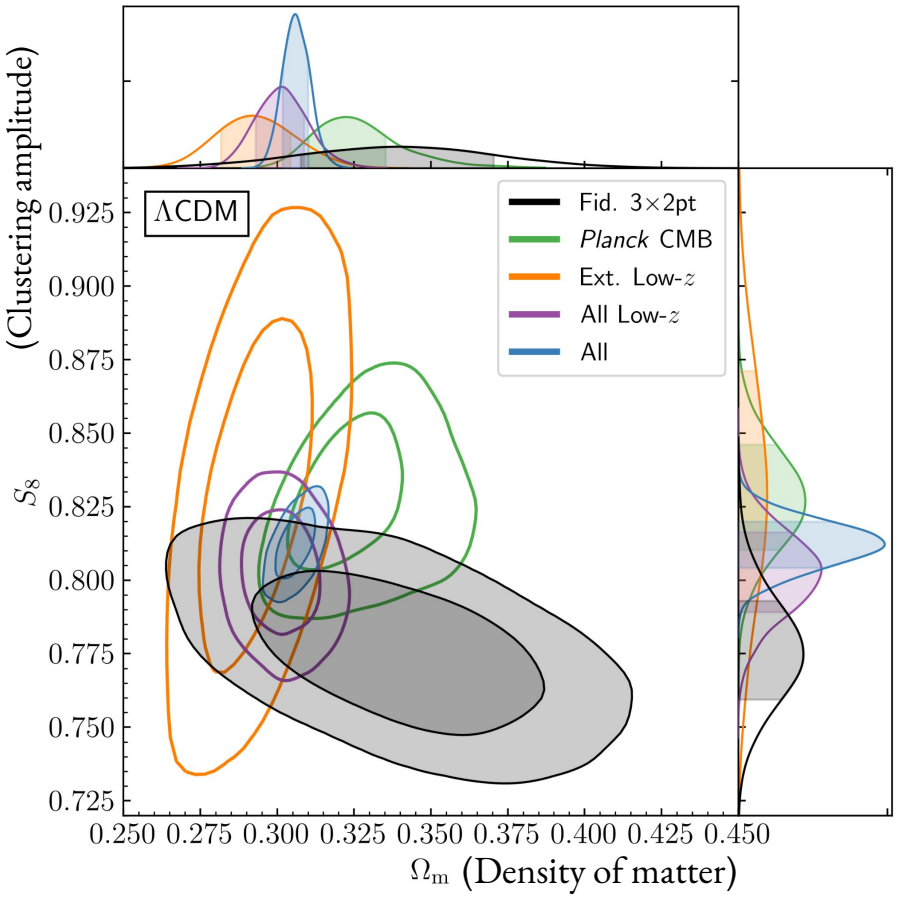

Key result: DES + External low z (SNe Ia, BAO, RSD) + CMB - tightest constraints

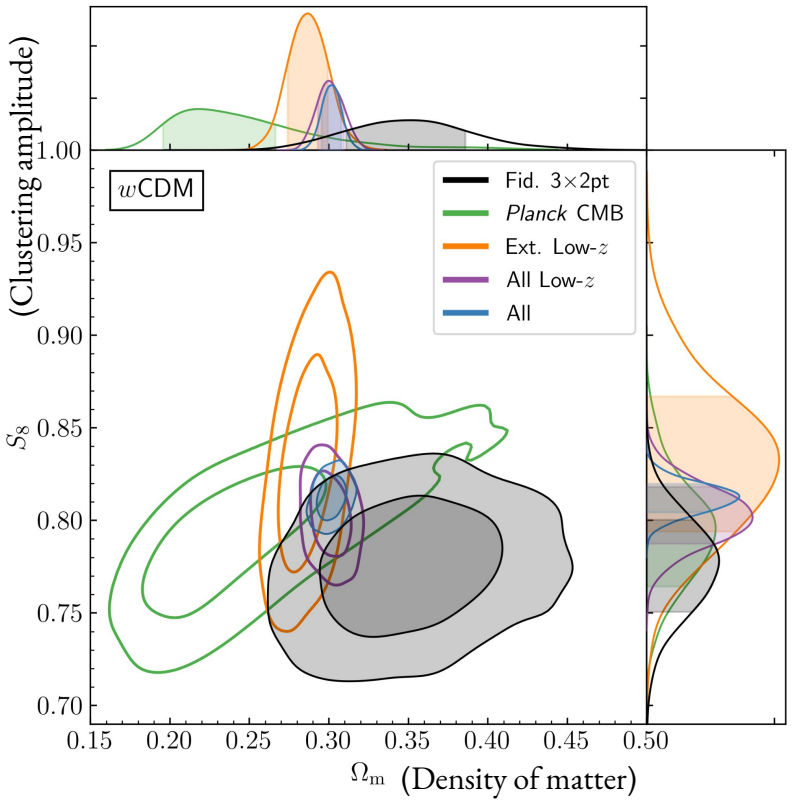

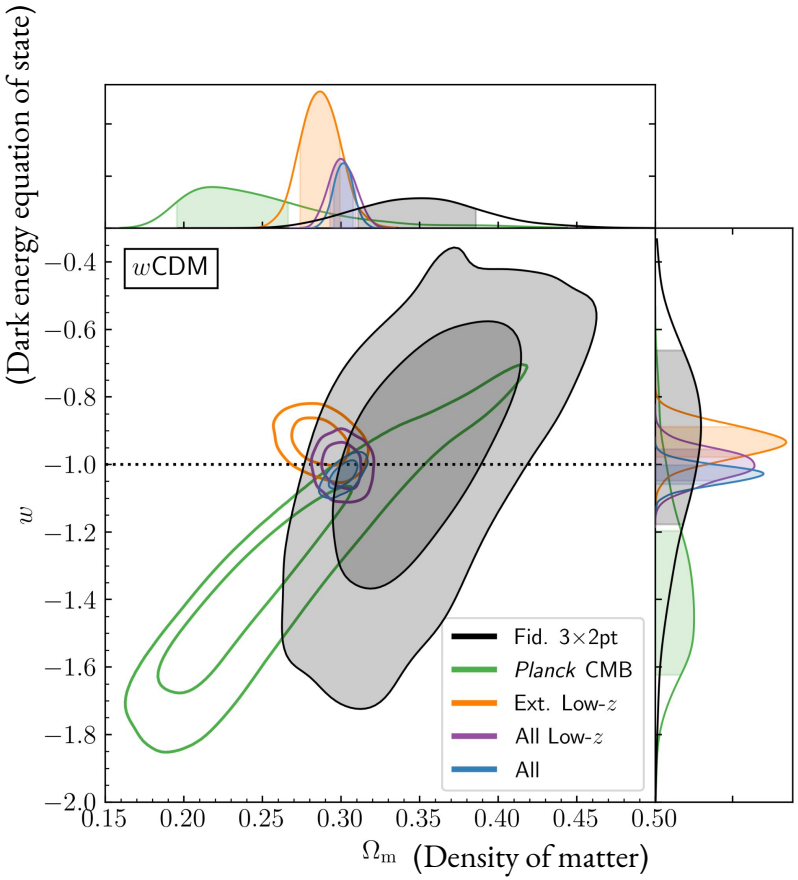

1) Cosmology from the angular BAO feature detection

Dark Energy Survey Year 3 results. List of key and supporting papers

1. “Dark Energy Survey Year 3 Results: Galaxy Sample for BAO Measurement” A. Carnero et. al.
2. “Dark Energy Survey Year 3 Results: Galaxy mock catalogs for BAO analysis”, I. Ferrero et. al. (2021)
3. “Dark Energy Survey Year 3 Results: A 2.7% measurement of Baryon Acoustic Oscillation distance scale at redshift 0.835”, DES Collaboration (2021)

BAO as a history of expansion probe

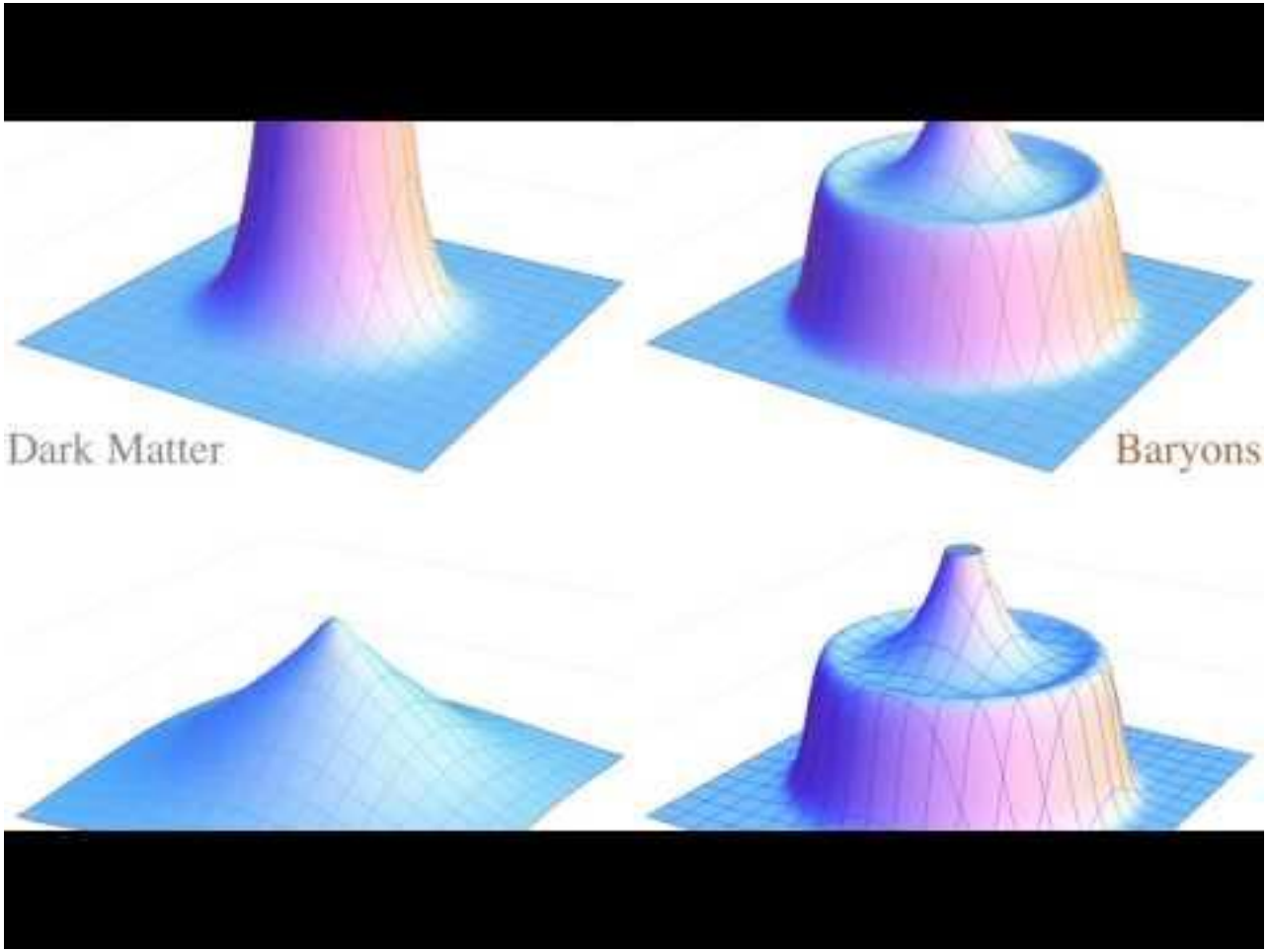

BAO as a history of expansion probe

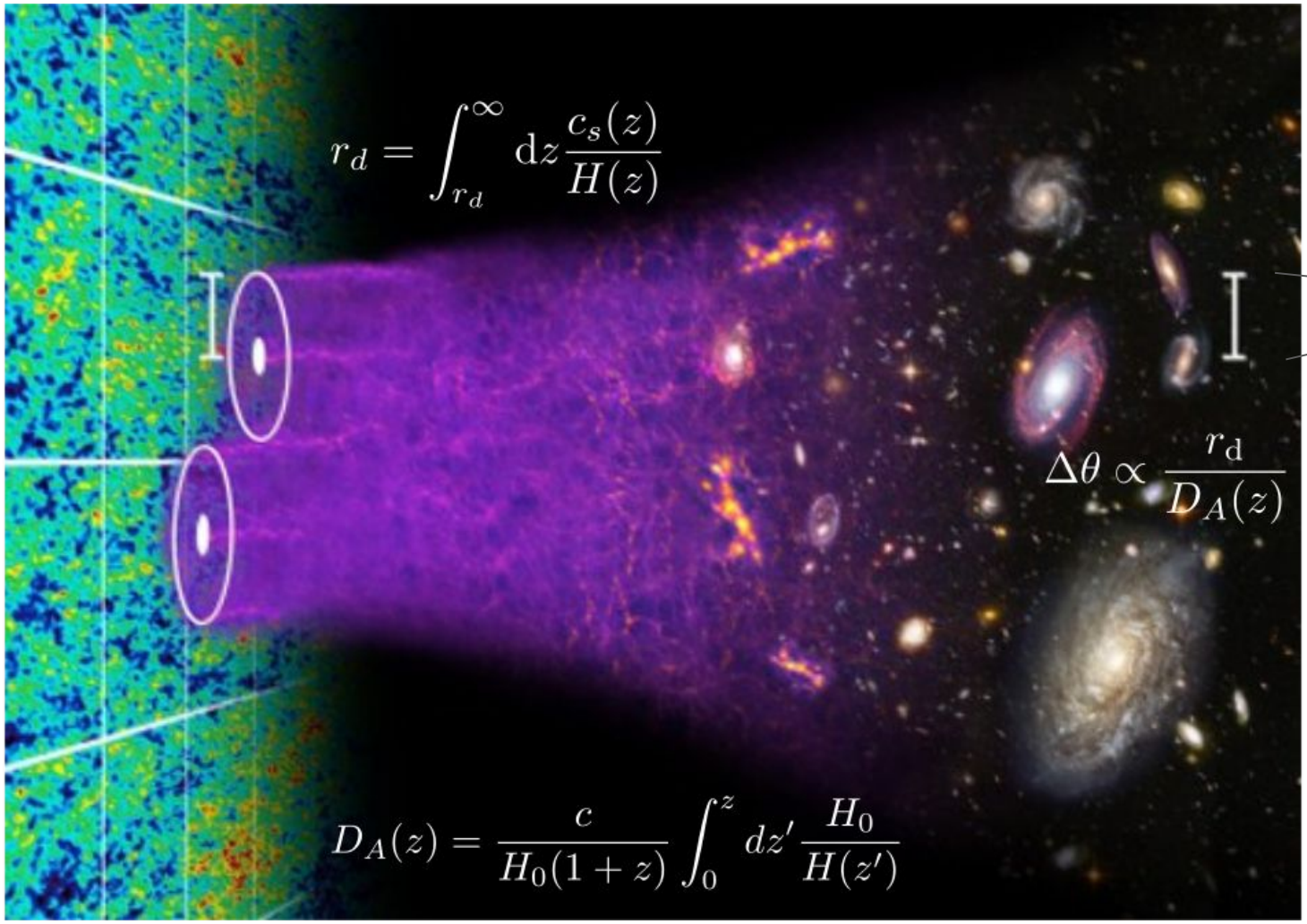

The BAO Sample

Red galaxies following color selection as in Y1.

- Balance the sample density with the photoz precision above redshifts greater than 0.5.
- 4108.47 deg2 , ~ 3 x Y1 BAO sample and has 7031993 galaxies in $0.6 < z < 1.1$, up to a magnitude limit of $i < 22.3$.

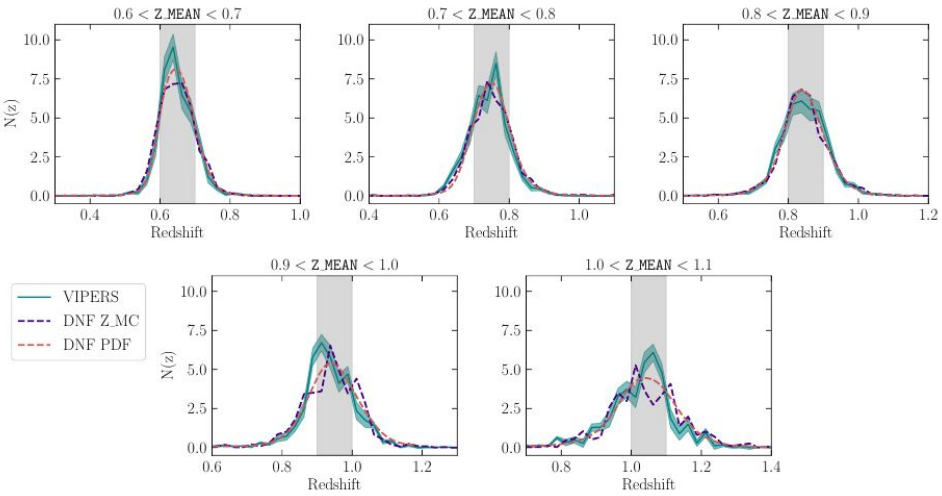

We split the sample into 5 tomographic bins.

Key difference from Y1: Adding the last higher z bin.

As for the lens samples, the same **Iterative systematics decontamination (ISD)** was applied to mitigate LSS systematics

Carnero et. al. (2021)

Clustering measurements

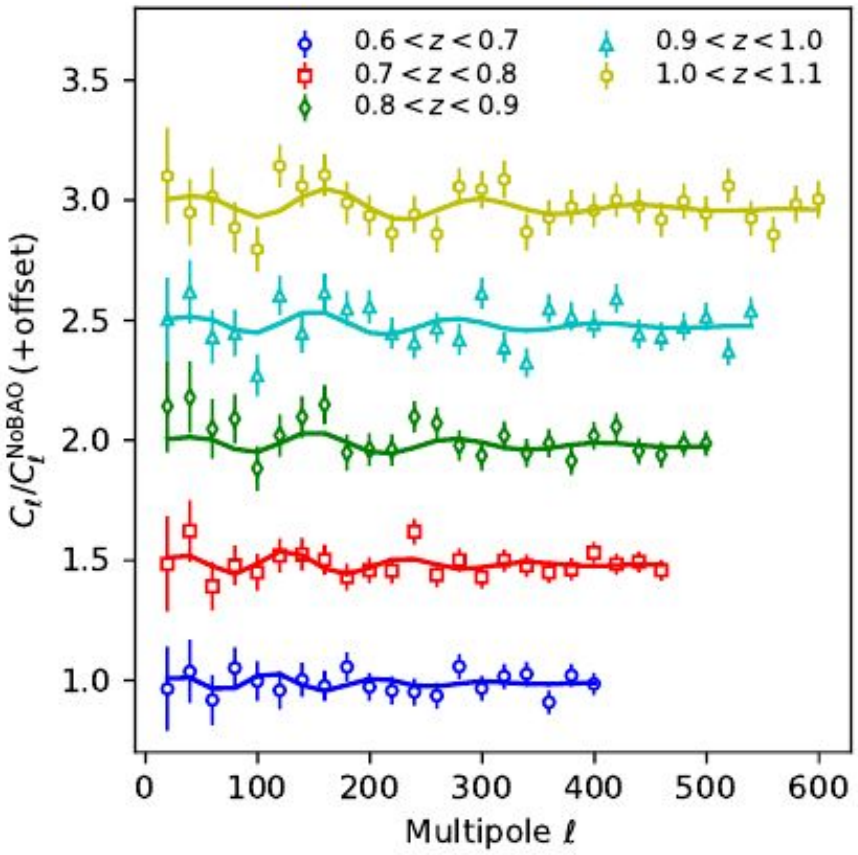

Angular power spectrum

Camacho et. al. (2019)

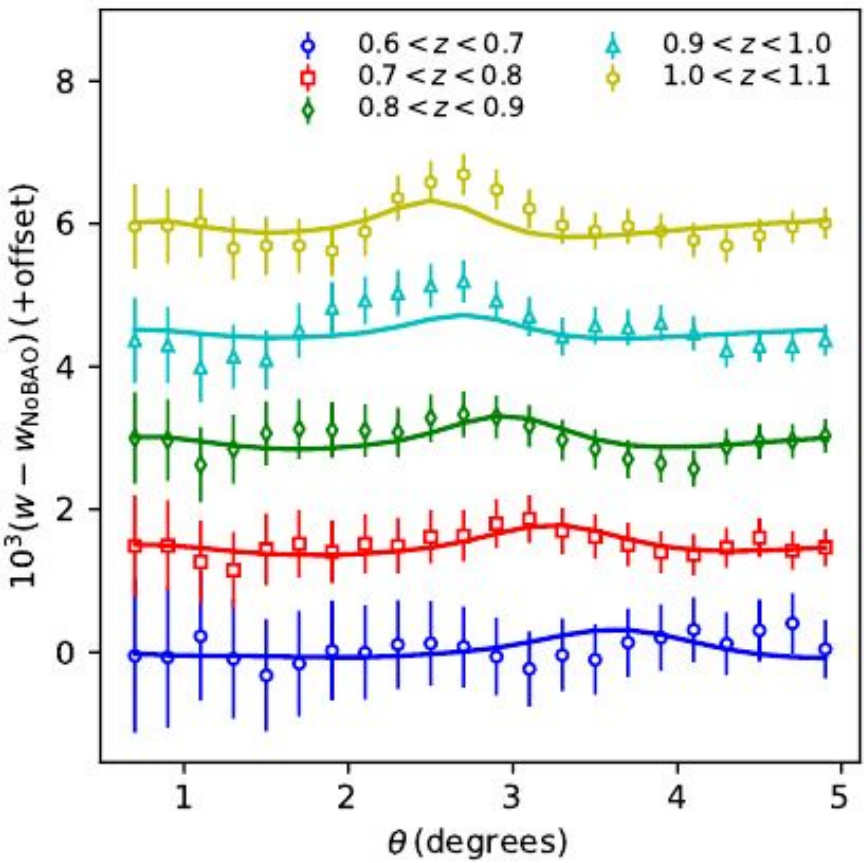

Angular correlation function

Chuen-Chan et. al. (2019)

From clustering measurements to the BAO feature

We are interested in the location of the BAO peak on the correlation function, not in its full-shape, we then use a template-fitting approach

- Configuration space
  $M(x) = BT_{\rm BAO}(x\alpha) + A(x)$
- Harmonic space
  $C(\ell) = BT_{\rm BAO}(\ell/\alpha) + A(\ell)$

Having a single parameter

$$\alpha = \frac{D_A(z_{\rm eff}) r_{\rm d}^{\rm fid}}{D_A^{\rm fid}(z_{\rm eff}) r_{\rm d}}$$

= $\Delta\theta$(BAO, fid) / $\Delta\theta$(BAO)

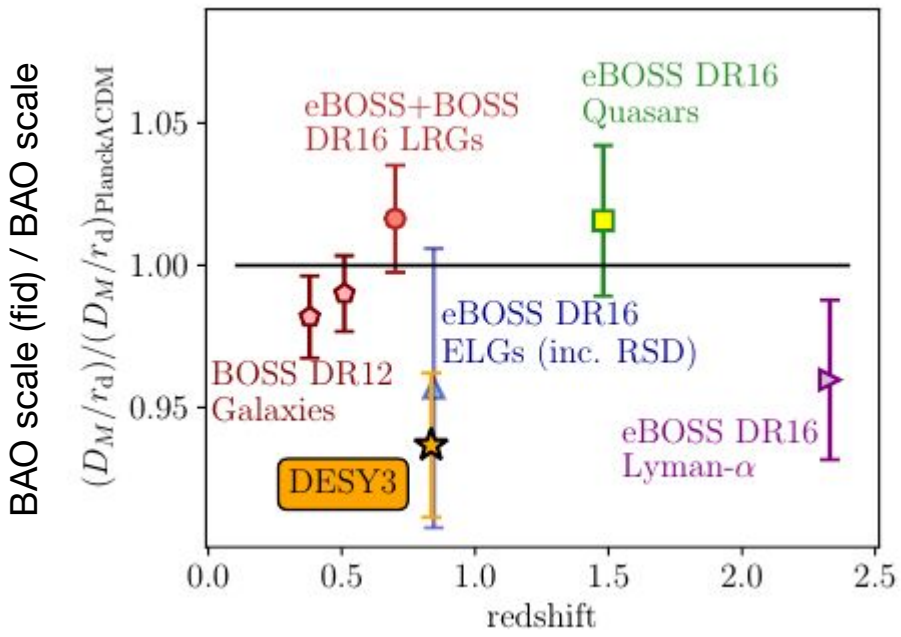

From clustering measurements to the BAO feature

We have benchmarked with two sets of mocks (~2000)

- FLASK: lognormal realizations
- COLA: Fast N-body (ICE-COLA) simulations populating halos with galaxies, using a hybrid Halo Occupation Distribution - Halo Abundance Matching model

(Avila et. al. 2019, Ferrero et. al. 2021)

And finally adopted as default, a halo-model based analytical covariance, COSMOLIKE (As the 3x2pt)

$$\chi^2(\boldsymbol{p}|\boldsymbol{d}) = \sum_{ij} \left[\boldsymbol{d} - \boldsymbol{M}(\boldsymbol{p})\right]_i C_{ij}^{-1} \left[\boldsymbol{d} - \boldsymbol{M}(\boldsymbol{p})\right]_j,$$

Combining the ACF and the APS

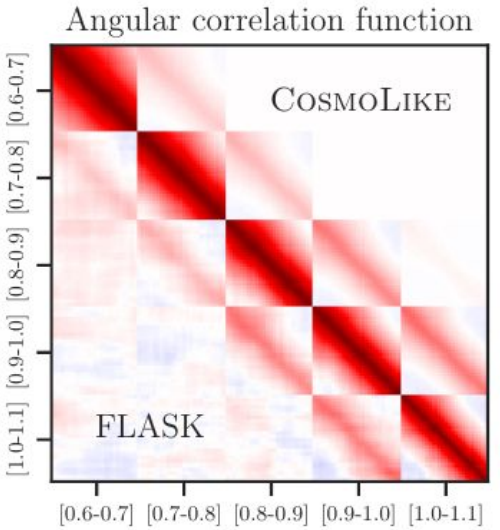

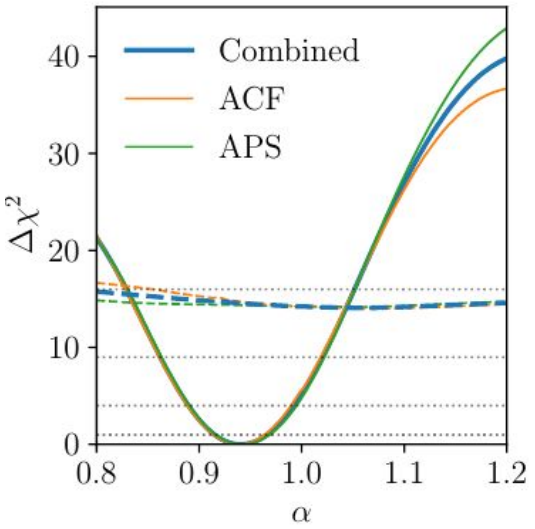

Key result: BAO Feature detection

2.7% detection at z=0.835 (Improved from 4% in Y1)

The most precise BAO distance measurement from imaging data to date. Competitive with the latest transverse ones from spectroscopic samples at z > 0.75

At a significance level of 2.3σ

Robust under a battery of tests specially designed for pre-unblinding procedure.

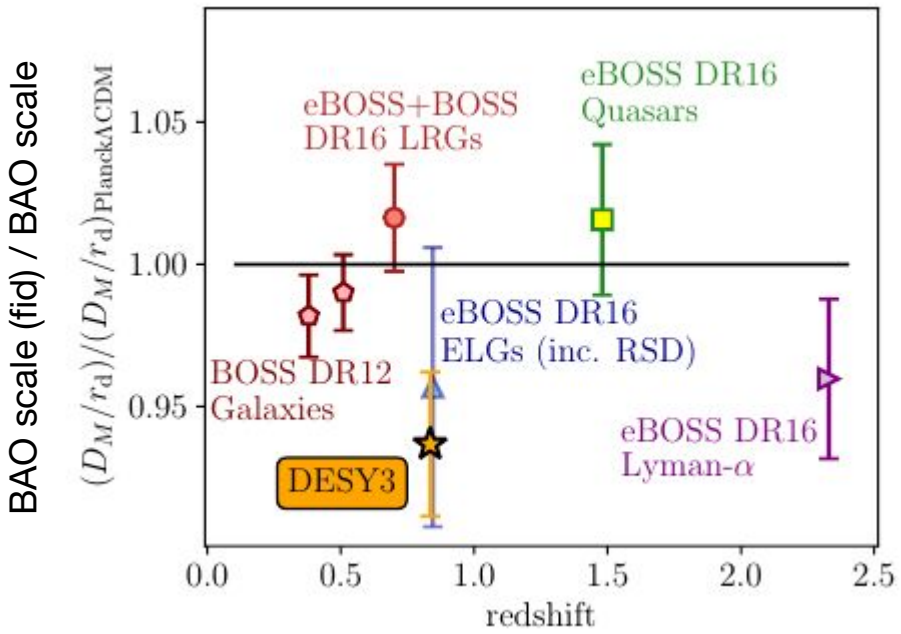

Y3 Measurement $z_{\rm eff} = 0.835$	$D_M/r_{\rm d}$ 18.92 ± 0.51	
case	α	χ^2/dof
$w(\theta) + C_\ell$ [method 1: **FID**]	0.941 ± 0.026	-
$w(\theta) + C_\ell$ [method 2]	0.939 ± 0.025	-
Robustness tests:		
$w(\theta)$	0.937 ± 0.025	95.2/89
$w(\theta)$ no sys	0.935 ± 0.026	94.6/89
$w(\theta)$ sys − PCA50	0.937 ± 0.025	94.9/89
$w(\theta)$ $n(z)$ DNF PDFs	0.935 ± 0.025	95.6/89
$w(\theta)$ $\theta_{\rm min} = 1^\circ$	0.939 ± 0.025	81.7/79
$w(\theta)$ $\theta_{\rm max} = 4^\circ$	0.937 ± 0.025	54.7/64
$w(\theta)$ $\Delta\theta = 0.1^\circ$	0.942 ± 0.026	220.2/204
$w(\theta)$ 2345	0.948 ± 0.026	67.8/71
$w(\theta)$ 1345	0.929 ± 0.026	80.7/71
$w(\theta)$ 1245	0.935 ± 0.028	78.4/71
$w(\theta)$ 1235	0.925 ± 0.028	70.0/71
$w(\theta)$ 1234	0.967 ± 0.026	82.3/71
C_ℓ	0.942 ± 0.026	92.3/99
C_ℓ no sys	0.940 ± 0.028	89.7/99
C_ℓ sys − PCA50	0.941 ± 0.026	89.7/99
C_ℓ $n(z)$ DNF PDFs	0.940 ± 0.025	92.1/99
C_ℓ $\ell_{\rm max} = 550$	0.940 ± 0.026	104.6/109
C_ℓ $\Delta\ell = 10$	0.939 ± 0.027	238.8/226
C_ℓ $\Delta\ell = 30$	0.936 ± 0.028	40.0/57
C_ℓ 2345	0.954 ± 0.028	82.2/84
C_ℓ 1345	0.938 ± 0.029	82.0/81
C_ℓ 1245	0.940 ± 0.028	79.5/79
C_ℓ 1235	0.932 ± 0.029	56.3/77
C_ℓ 1234	0.961 ± 0.029	69.1/74

Key result: 3x2pt + History of growth from DES

Pure history of growth constraints from DES are consistent with 3x2pt and can be combined to have

$$h = 0.691^{+0.138}_{-0.043},$$
$$\Omega_m = 0.344^{+0.029}_{-0.025},$$
$$S_8 = 0.773^{+0.018}_{-0.019},$$

$$h = 0.72^{+0.090}_{-0.053},$$
$$\Omega_m = 0.317^{+0.021}_{-0.020},$$
$$S_8 = 0.778^{+0.016}_{-0.017}.$$

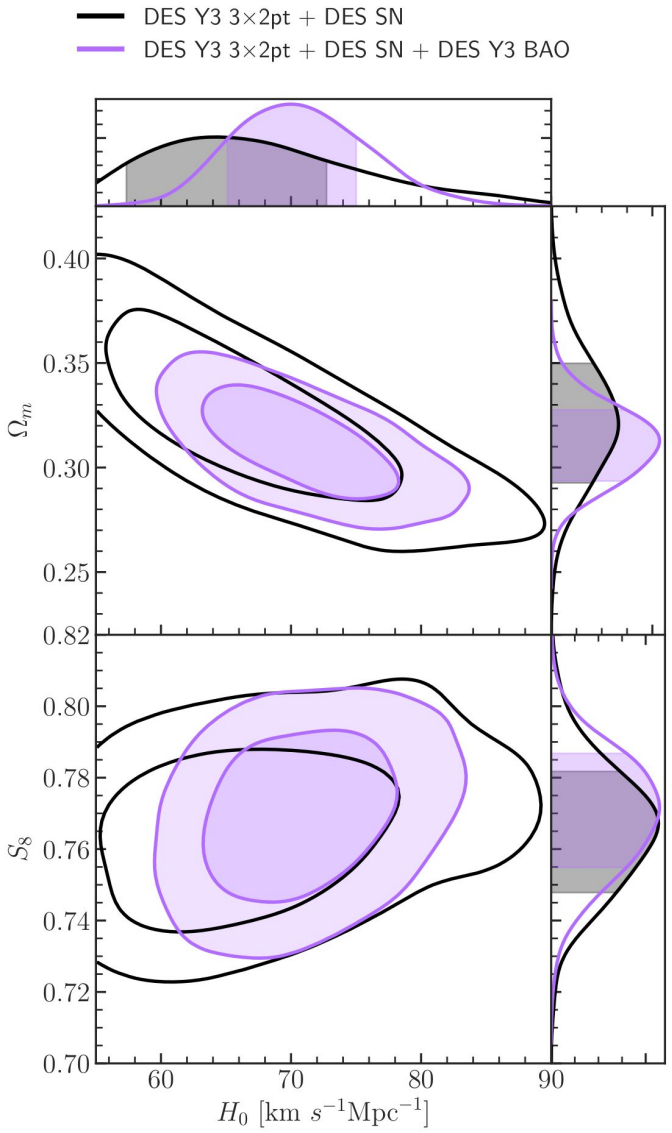

Key result: 3x2pt + History of growth from DES

Consistency with Planck is maintained.

Combination with DES 3x2pt + SNIa, they lead to improvements in H0 and Ωm constraints by ~ 20%.

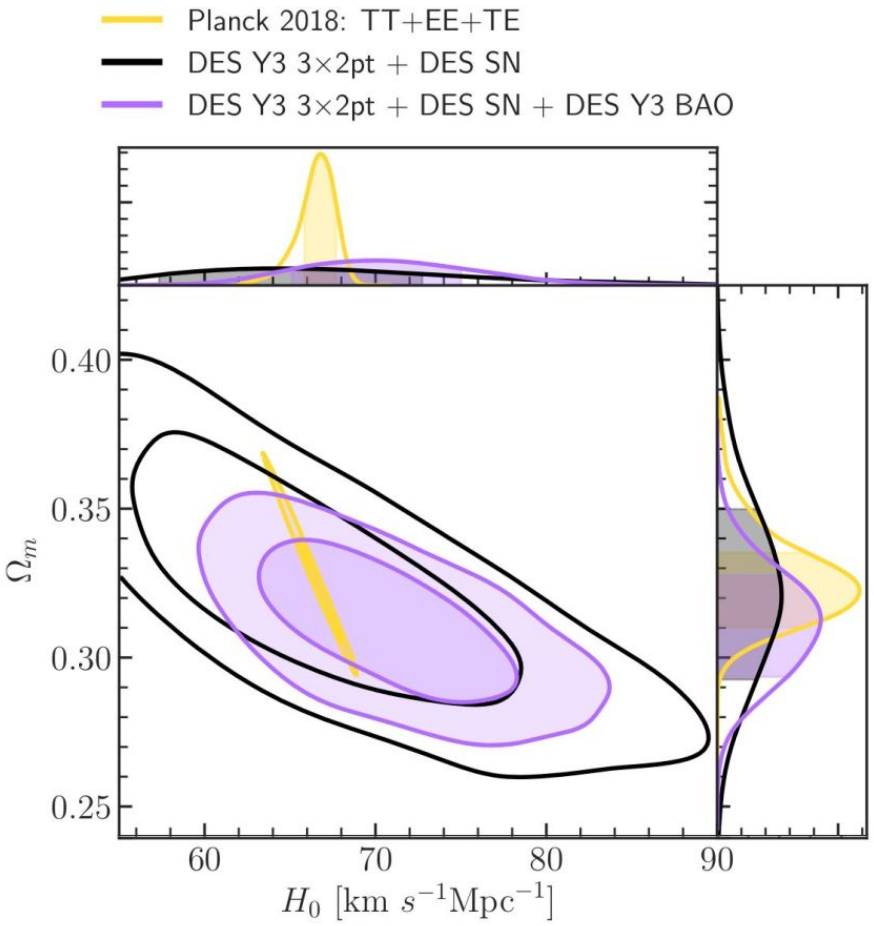

Summary and conclusions

We've presented a brief overview of some of the **novel methods** and advancements necessary to **fully utilize the statistical power of the DES Y3 data**.

We find a **slightly higher clustering amplitude and matter density than in DES Y1 3x2pt**. We have improved the signal-to-noise of the 3x2pt measurement by a **factor of 2.1** from DES Y1.

We find and improved **2.7% detection of BAO feature** from the 4% in DES Y1.

We find **no significant evidence for inconsistency in ΛCDM** between DES and *Planck*, or between DES + other complementary low-redshift probes and *Planck*.

Combining **3x2pt + SNIa from DES with BAO results can allow to improve DES-only constraints in h and Ωm in ~ 20%** being an interesting avenue of research for future photometric surveys.